A DESCRIPTION OF THE PHYSICAL OCEANOGRAPHIC FEATURES OF THE EASTERN GULF OF MEXICO, AUGUST 1968

by

Michael John Schneider

A DESCRIPTION OF THE PHYSICAL OCEANOGRAPHIC FEATURES OF THE EASTERN GULF OF MEXICO, AUGUST 1968

A Thesis

by

Michael John Schneider

Submitted to the Graduate College of
Texas A&M University in
partial fulfillment of the requirement for the degree of

MASTER OF SCIENCE

August 1969

Major Subject Physical Oceanography

ABSTRACT

A Description of the Physical Oceanographic Features of the Eastern Gulf of Mexico, August 1968. (August 1969)

Michael J. Schneider, B. S., U. S. Merchant Marine Academy

Directed by: Dr. Luis R. A. Capurro

A three week cruise in the Gulf of Mexico in the late summer of 1968 provides the basis for a report on water masses, circulation, geostrophic transport, sea surface temperature data, and sound velocity conditions found there. The Caribbean water is the source of water flowing north through the Yucatan Strait and into the Gulf. Two distinct T-S relationships are found in the eastern Gulf for the upper layers above 17°C. Water characterized by the T-S curve similar to that of the Caribbean water is termed right-hand water and the water identified by the other T-S curve is called left-hand water. These names are consistent with the location of these waters in respect to the side of the current on which they are found. Water flowing north through Yucatan Strait becomes a loop circulation pattern that exits through Florida Straits. This current carries 46.7 million m^3/sec of water into the Gulf and forms a large anticyclonic eddy centered near 25.5°N and 87.0°W. The values of geostrophic transport computed are among the highest ever reported here. The sea surface temperature field is found to have sharp gradients near each side of the loop current. A band of surface

water about 40 kilometers wide lying at the surface of the loop current is 0.3 to 1.1°C colder than the surrounding water. The two distinct T-S curves found in the eastern Gulf result in sound velocity conditions that are significantly different for the right- and left-hand water. The nature of these differences is discussed as well as daily and seasonal variations in the sound velocity profile.

ACKNOWLEDGMENTS

I wish to express my appreciation to Dr. Luis R. A. Capurro for his guidance in the preparation of this thesis and for his enthusiasm and personal interest in my education at Texas A & M University. I am also grateful to Dr. Dale F. Leipper who suggested this topic and who first aroused my interest in the current patterns in the Gulf of Mexico. Dr. William S. McCulley has also been very helpful in the preparation of this work.

I am indebted to Mrs. Rosemary Boykin, Mrs. June Hagler, and Miss Margaret Donovan for their valuable assistance in the preparation of this manuscript, and to Mr. Hector Cornelio who did the major part of the drafting.

Special thanks go to Mr. William Merrell who has offered many helpful ideas and suggestions during the course of this research dating back to the cruise itself and continuing through the analysis of the data and the composition of the thesis.

TABLE OF CONTENTS

LIST OF TABLES

LIST OF FIGURES

CHAPTER I

INTRODUCTION

Historical Remarks

Although several hydrographic surveys were made in the Gulf of Mexico in the late 1930s and 1940s, the results did not completely describe the field of motion and its variations (Leipper, 1954). Austin (1955) first reported indications of a large scale anti-cyclonic eddy at the surface centered at approximately 26°N and 86°W in August and September, 1954. He postulated that this was a semi-permanent feature that changes in size, shape, and intensity in time and space. Insight into some of the physical properties of water in the Gulf of Mexico can be gained by studying the water in the Caribbean Sea since this is the source of the Yucatan Current water. Wust (1964) has presented a detailed descriptive analysis of the water in the Caribbean Sea as far north as Yucatan Strait. The dynamics of circulation and geostrophic transport computations in the Caribbean have been reported by Gordon (1967). Investigations by Cochrane (1961, 1963, and 1965) have described the Yucatan Current at its source and as it flows through the Yucatan Strait.

Within the Gulf of Mexico, Nowlin and McLellan (1967) have reported the circulation patterns in the winter of 1962 which they suggest are typical of the winter circulation. They have stated

---

The citations on the following pages follow the style of the Journal of Geophysical Research.

that a loop current in the eastern Gulf of Mexico is the main feature of the surface circulation. This loop current enters the Gulf through the Yucatan Strait and exits through the Straits of Florida.

In the eastern Gulf of Mexico, eight brief cruises were conducted between May, 1964, and February, 1968, by Leipper to investigate the circulation by studying the thermal structure. The loop current was crossed a total of 40 times during these cruises and on three other cruises for which data were available. Leipper (1967), reporting on this data, described a sequence of current patterns with an apparent seasonal variation. He stated that this current transported some 25 to 45 million m^3/sec of water at speeds up to 2.05 m/sec (4 knots). Leipper believed that the shape and size of the basin play an important role in the circulation but that normally the local winds and weather do not. Birchett (1967) has studied the shallow (above 300 meters) circulation in the Gulf of Mexico as indicated during one of the cruises of this series and has commented on the use of the salinity/temperature/depth (STD) continuous profile recorder in this type of quasi-synoptic oceanographic surveying.

Cruise Objectives

This cruise (68-A-8) was to be the last of the series of cruises under the direction of Dr. Leipper to study the circulation in the eastern Gulf of Mexico where the loop current had been found. These cruises had been scheduled in the early spring and in the late

summer to survey the conditions during the coldest and warmest times of the year. The purpose of the cruise was to delineate the water masses present in the eastern Gulf, to define the loop current using temperature/depth relationships and dynamic computations, and to check for the presence of any detached eddy such as had been found in August, 1965, (Leipper, 1967) and in June, 1967, (Nowlin, Hubertz, and Reid, 1967). During the period of the cruise, a NASA research aircraft was scheduled to fly over the area of the loop current (test site 173) using different types of remote sensors. It was expected that these data would be used to provide additional information for the analysis of the loop. Therefore, it was necessary for the cruise to obtain good sea surface reference data (ground truth) with which to calibrate the remote sensed data.

Subsequent to the cruise, additional investigations were conducted concerning sound velocity conditions and remote sensing of sea surface temperature. Adequate data to support this work had been collected on the cruise. Charts showing sea surface temperature field were prepared to provide ground truth data and to be used in the sound velocity study. These also provided a basis for comparing sea surface temperature data gathered by remote sensing techniques with that obtained in the classical manner.

Cruise Planning

Cruise 68-A-8 was planned to be a quasi-synoptic survey of the eastern Gulf of Mexico to provide additional information on the

sequence of currents there and to complete the spring and fall data reports by Dr. Leipper. To accomplish this objective, hydrographic stations were to be taken at 30 nautical mile intervals with bathythermograms (BTs) to be taken hourly between stations. The hydrographic station casts were to be taken to 1200 meters or to the bottom in shallower water. In addition to the mechanical BTs, a number of expendible BTs (XBTs) were available which provided temperature/depth information to 450 meters. The cruise plan was flexible enough to permit the investigation of any unusual features or of a detached eddy, should one be found.

Originally, one port stop was scheduled at Progreso, Mexico, near the middle of the three week cruise. Three days after leaving Galveston, operational considerations required that the ship put in to New Orleans, Louisiana. The result of this change in plan was that the remainder of the cruise, which was in the area of primary interest, was conducted without interruption, thereby covering the area in the shortest possible time.

CHAPTER II

OBSERVATION

Field Work

The survey of the eastern Gulf and fixing the position of the Gulf loop current was started at the time of departure from South Pass of the Mississippi Delta (approximately 2200 GMT on August 22, 1968). During the next 10 days and 3 hours, R/V ALAMINOS steamed 2270 nautical miles, occupied 62 stations, and took 187 BTs and XBTs. Following station 73 (0126 GMT on September 2, 1968), the ship surveyed a portion of the north central Gulf of Mexico returning to Galveston on September 5, 1968.

In the eastern Gulf, the cruise plan (Figure 1) had been laid out to cross the loop current on a number of legs that were normal to the configuration of the loop based on its expected position for this time of year. These legs, called transects, were approximately 60 nautical miles apart. At the eastern end, the transects were terminated at the 100 fathom (183 meter) curve as determined by the precision depth recorder (PDR). At the western end, the southern 3 transects continued to the 100 fathom curve off Campeche Bank. All the transects except the one in Yucatan Strait were approximately 220 nautical miles long. One long leg oriented parallel to the axis of the expected loop and bisecting it was surveyed to determine the northern extent of the loop and to investigate the possibility of a

Figure 1

Cruise track 68-A-8. (After Leipper, 1968e)

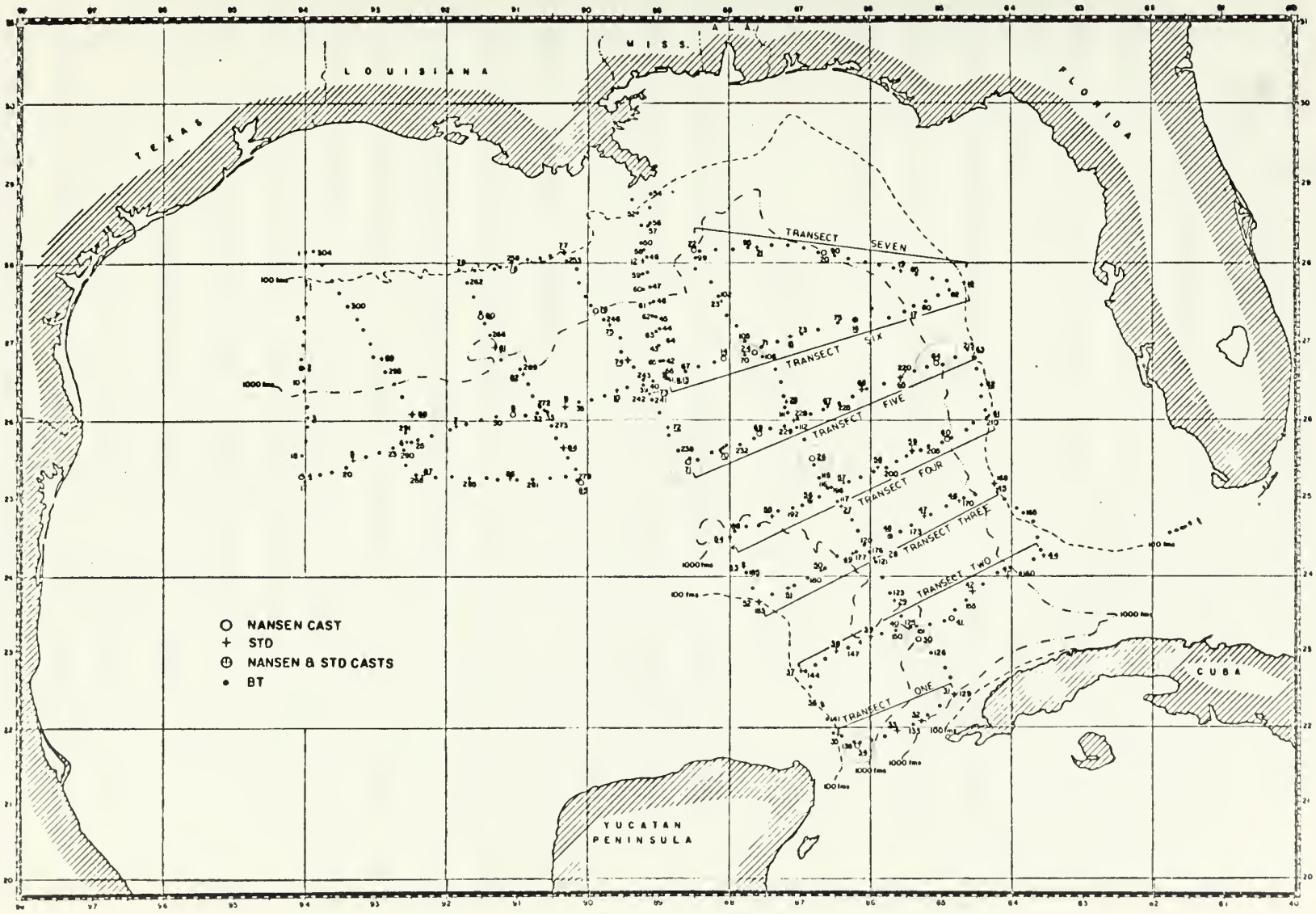
TEXAS
LOUISIANA
MISS.
ALA.
FLORIDA
CUBA
YUCATAN PENINSULA
TRANSECT SEVEN
TRANSECT SIX
TRANSECT FIVE
TRANSECT FOUR
TRANSECT THREE
TRANSECT TWO
TRANSECT ONE
100 fms
1000 fms
NANSEN CAST
STD
NANSEN & STD CASTS
BT

detached eddy.

Although no survey of this type is truly synoptic, it is felt that the effects of time variation were at a minimum on this cruise. The entire eastern Gulf of Mexico in the area of the loop current was surveyed in about 10 days. This is an acceptable interval when attempting to define a current that may have a seasonal variation. The values of the topography of selected isotherms, the subsurface salinities, and the dynamic topography were similar when cruise legs crossed each other at different times.

Data Collection and Processing

A Hytech model 9006 salinity/temperature/depth (STD) continuous profile recorder was used as well as classical hydrocasts with Nansen bottles and paired reversing thermometers at hydrographic stations. STD data points were extracted from the digital records at or near the standard depths and then handled in the same manner as the Nansen data. The STD analog record was used only for visual identification of the water mass and to see at a glance the vertical distribution of temperature and salinity. Station observations included 22 Nansen casts and 68 STD casts. At station 56, both types of cast were taken. Temperature/salinity curves for all stations were drawn as soon as possible after leaving the station. This provided an early check of the data, and would have drawn attention to unusual features that might merit further investigation.

A BT was taken hourly between stations and of the total of 304,

there were 90 XBTs. Surface temperature and salinity samples, taken by bucket, provided supplemental information for checking surface STD measurements and BTs. The mechanical BTs were corrected for depth and temperature errors by applying the mean values of the depth error and surface temperature error as determined from the BT grid reference and the bucket temperature respectively. For the XBTs, the surface reference is established when the probe enters the water and the electrical circuit that starts the recorder is completed. Each XBT was read after the trace was adjusted to the zero reading on the graph.

No correction for surface temperature was made to XBTs for two reasons. First, the mean difference between bucket and XBT surface temperature is -0.05°C which is almost insignificant considering the precision to which both the XBT and bucket thermometers are read. Second, the XBTs were used only to determine the depth of isotherms. If the XBTs had been adjusted to the bucket temperatures, the resulting difference in the depth of the 22°C isotherm would have been less than 6 meters, and this made no difference in the interpretation of the data.

Continuous temperature and salinity recordings were made by direct sampling from a sea water intake at a nominal depth of 3 meters below the surface. Temperature measurements were made by resistance thermometer and salinity was measured by an inductive salinometer. A Barnes infrared thermometer (IRT) was mounted on the bow of the ship and positioned to measure the skin temperature of

the sea surface about 5 meters forward of the bow wake and slightly to one side.

Salinity determinations of all water samples were carried out utilizing a shipboard conductive salinometer (University of Washington, #12). Dissolved oxygen concentrations were determined for the water samples taken on Nansen casts using the Carpenter (1965) method. Percentage of saturation of dissolved oxygen was determined from the tables by Green and Carritt (1967). Weather observations were made at 6 hour intervals and logged on standard U. S. Weather Bureau forms.

The STD digital recording system failed on stations 13, 36, and 65. The data from the analog recorder were not used in place of the digital data at these stations because of the poor quality of the analog record and because of the desire to maintain a consistent procedure in data handling techniques. Therefore, no data are presented for these three stations.

Station data were reduced using the Leipper Version of Oceanographic Data Program F. This program has been revised from its original form to make it compatible with the IBM-360 computer at the Data Processing Center, Texas A & M University. This program employed a Lagrangian interpolation scheme to compute temperature and salinity at standard depths. Values of sigma-T, thermosteric anomaly, dynamic height, sound velocity, and geostrophic transport function were then computed for standard depths. (A copy of this program appears in Leipper, 1968c.)

CHAPTER III

WATER MASSES

T-S Diagrams

The strong flow of water northward through Yucatan Strait, the semipermanent anticyclonic eddy, and the outflow toward the Florida Straits will be referred to here as the Eastern Gulf Loop Current or simply as the loop current. Unless it is stated to the contrary, temperature is in degrees Centigrade (°C), salinity is in parts per thousand ($^{o}/oo$), depth is in meters (m), velocities are in meters per second (m/sec), dissolved oxygen is in milliliters per liter (ml/l), thermosteric anomaly is in centiliters per metric ton (cl/t) and time is Greenwich Mean Time (GMT). This paper is the result of a study of the data from R/V ALAMINOS cruise 68-A-8 and the findings are only representative of the period August 17, 1968, to September 5, 1968, unless otherwise stated.

The water flowing into the Gulf through Yucatan Strait comes from both the North and South Atlantic Oceans. The water mixes in the Caribbean Sea as it flows westward and then northward toward the Yucatan Strait. The upper waters in the Caribbean are mainly of North Atlantic origin whereas the waters near the depth of the salinity minimum (600 to 800 meters) are predominantly of South Atlantic origin (Sverdrup, et al., 1942). The temperature/salinity (T-S) curve for the water south of Yucatan Strait indicates the

presence of four distinct water masses. Listed in order of increasing depth, they are: the Surface Water which occurs down to the top of the seasonal thermocline, the Subtropical Underwater (SUW), the Subantarctic Intermediate Water (SIW), and the North Atlantic Deep Water (NADW).

Figure 2 shows the temperature/salinity (T-S) relationship observed on cruise 68-A-8. The figure is a composite of T-S data points from 27 selected stations in the eastern Gulf of Mexico. Stations 25, 26, 49, 50, 55, 56, 57, 66, 67, 68, 69, and 70 are shown by open circles and stations 14, 17, 24, 29, 30, 34, 37, 38, 40, 52, 53, 54, 59, 64, and 71 by the solid circles. The uniformity of the curve below 17°C indicates that the Gulf of Mexico waters comprise essentially one system (Nowlin and McLellan, 1967). Similar T-S curves have been previously reported by a number of investigators including Leipper (1967) and Birchett (1967). The minimum salinity, 34.85°/oo, which appears in the eastern Gulf at a temperature of approximately 6.3°C, is a remnant of the Subantarctic Intermediate Water. This part of the T-S curve is also similar to the one found in the Caribbean by Wust (1964: figure 3). This is consistent with the flow of Caribbean water into the Gulf through the Yucatan Strait.

Above 17°C, two separate T-S relationships are found. The T-S curve in Figure 2 having a salinity maximum of 36.73°/oo near a temperature of 22.5°C is very similar to the T-S curve found by Wust (1964: figure 3) for Caribbean waters. This salinity maximum

Figure 2

Temperature versus salinity for stations in the eastern Gulf of Mexico, cruise 68-A-8.

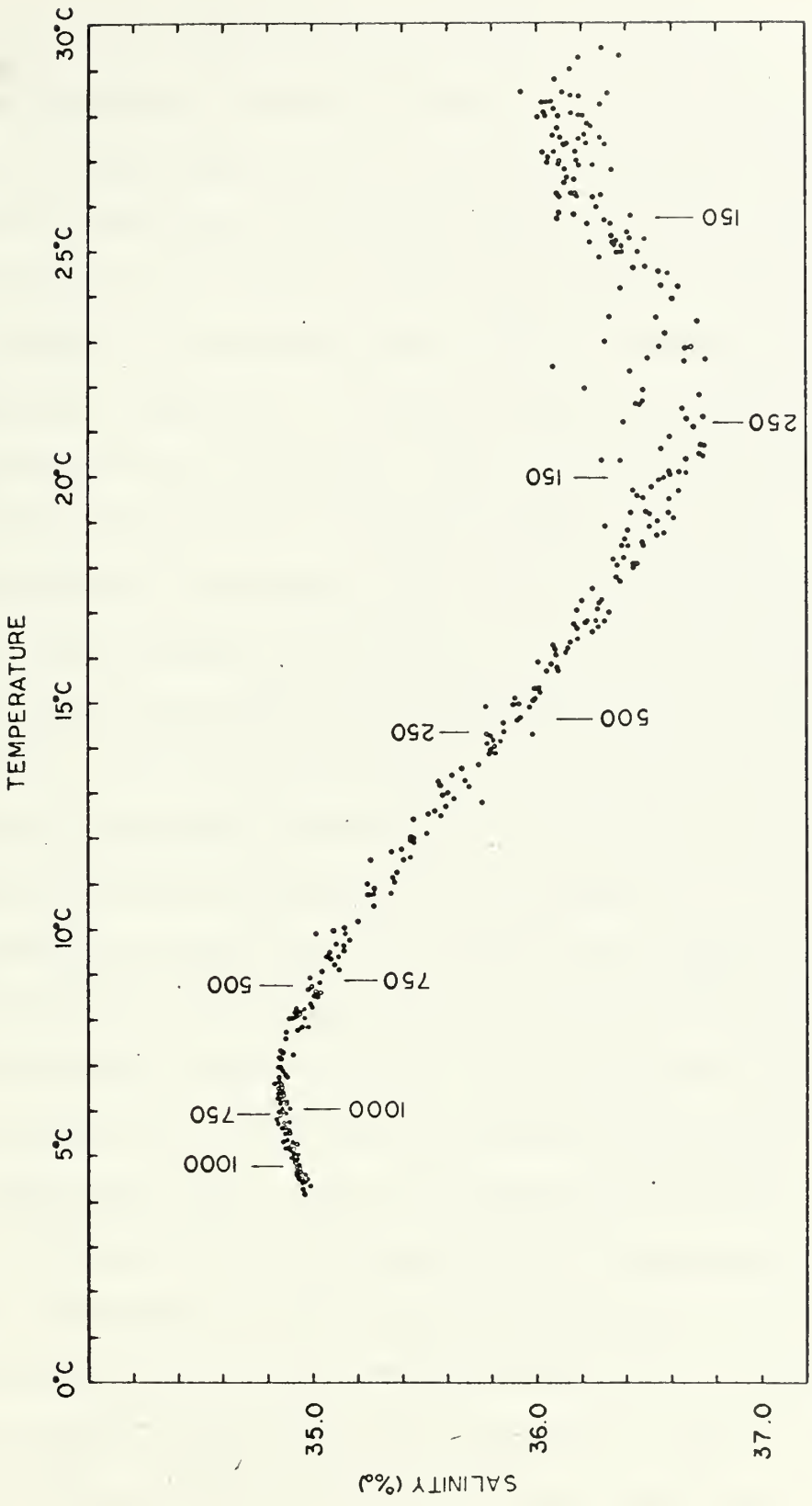
TEMPERATURE
0°C
5°C
10°C
15°C
20°C
25°C
30°C
35.0
36.0
37.0
SALINITY (‰)
150
250
150
500
250
750
500
1000
750
1000

is found at about 200 meters and represents the core of the Subtropical Underwater in the Gulf of Mexico. The water characterized by this T-S curve (open circles in Figure 2) is found to the right of the loop current when looking downstream and will be called right-hand water following the terminology of Leipper (1967).

The other T-S relationship has a salinity maximum at lower salinities and temperatures. A maximum salinity of 36.58°/oo was found near a depth of 100 meters. This T-S curve (solid circles in Figure 2) is characteristic of the water found to the left of the loop current and, accordingly, will be called left-hand water. Cochrane (1965) suggests that this part of the Yucatan Current flows inside Cozumel Island and Arrowsmith Bank which leads to the possibility of vigorous vertical mixing in this part of the passage. This feature may explain the difference in T-S curves in the right- and left-hand waters in the eastern Gulf of Mexico.

Although the shape of the T-S curves is quite similar below 17°C, the depth of water represented by a point on this portion of the curve is about 250 meters less in the left-hand water than in the right-hand water. This can be seen when plotting the T-S curves from summary sheet data. The depth represented by a point on the curve is indicated for both the right- and left-hand water in Figure 2. The depths for right-hand water are those at station 26 and appear below the T-S curve while the depths for the left-hand water are those of station 71 and appear above it. This is an indication of the adjustment of the field of mass to the existing flow.

In the right-hand water, the bottom of the seasonal thermocline is marked by a sharp inflection near 40 meters. This sharp inflection is found at a shallower depth in the left-hand water or may be missing completely. At this time of year (August and September) the mixed layer depths are generally the shallowest of the year. During the winter, they may extend down to 150 meters in the right-hand water.

For this cruise, the stations were initially classified as right- or left-hand water by inspecting their T-S curves. It was found that the portion of the curve between 150 and 250 meters would provide a reliable 'yardstick' for this classification. In this region of the water column, the shape and slope of the curves are different as well as the ranges of temperature and salinity. This classification scheme in the water above 250 meters makes it possible to derive a temperature/depth relationship that could be used to classify water from the BT data alone. Points on the lower portion of the T-S curve are found at depths 250 meters less in the left-hand water and this fact was used to verify the station classification in the deeper part of the water column.

The stations were classed as being right-hand, left-hand, mixed (between the values of the right- and left-hand water), and coastal. Coastal water did not refer to special T-S relationships but included the stations influenced by fresh water runoff or by the shallow depths of the continental shelf where the T-S curve differed significantly from that normally found in the right- and

left-hand water. Water classed as coastal water was found in the shallow waters around the edge of the Gulf and in the area effected by the Mississippi River outflow. Figure 3 shows the distribution of the water classed in this manner. The designation of left-hand water in the western Gulf is based solely on the classification of the T-S curve and no attempt is made to infer any circulation pattern in this area.

Dissolved Oxygen

The vertical distribution of dissolved oxygen, Figures 4 and 5, show marked differences for the right- and left-hand water. Similar profiles have been observed by Nowlin and McLellan (1967: figure 6) and reported by Van Schuyler and Hunger (1967: figure 13) although each paper refers to the right- and left-hand water by a different name. The vertical distribution of dissolved oxygen below the top of the thermocline shows little variation with time based on these data.

In August, 1968, concentrations of dissolved oxygen in the surface water were always at or near saturation for the particular temperature and salinity. In the right-hand water, a dissolved oxygen maximum (4.9 to 5.1 ml/l) is found near the top of the thermocline at about 75 meters where the concentrations are super-saturated. The dissolved oxygen minimum of 2.9 ml/l (44 percent of saturation) is found near 800 meters.

In the left-hand water, the surface values are also at or

Figure 3

Distribution of right-hand water, left-hand water, and mixed water, cruise 68-A-8. Shaded area indicates the mixed water.

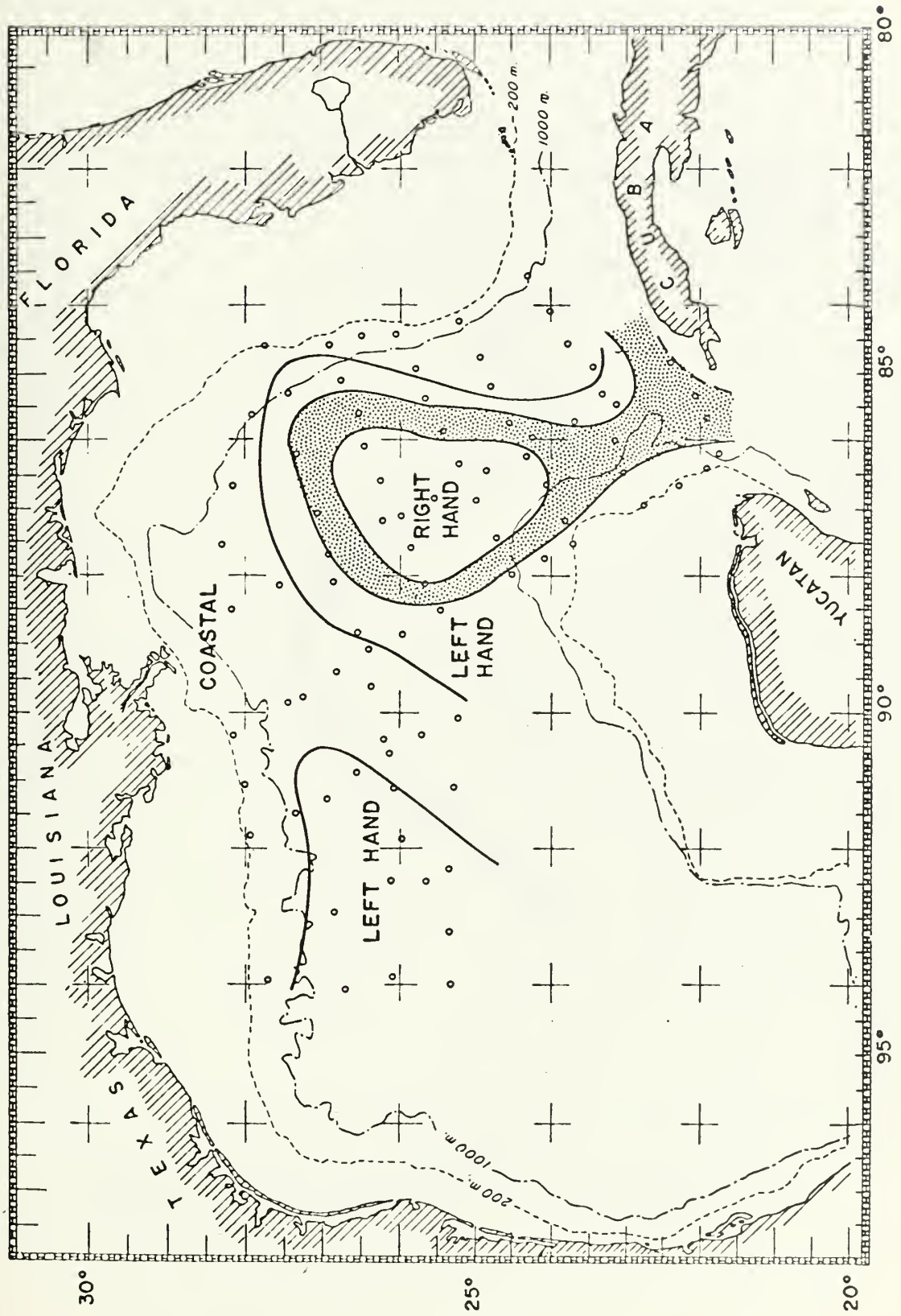
FLORIDA
LOUISIANA
TEXAS
YUCATAN
COASTAL
RIGHT HAND
LEFT HAND
LEFT HAND
200 m.
1000 m.
200m.
1000m.
A
B
C
80°
85°
90°
95°
30°
25°
20°

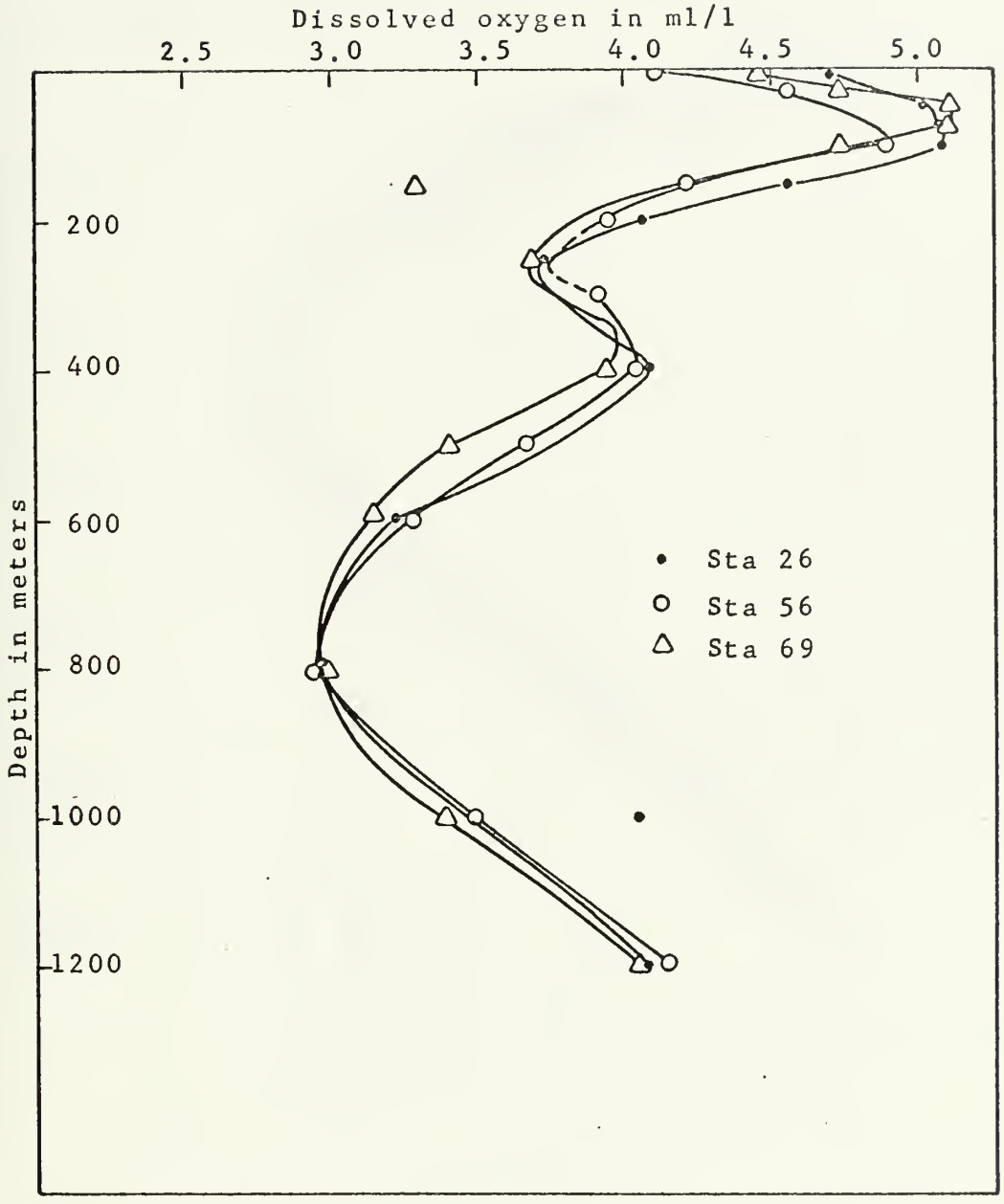

Figure 4
Vertical distribution of dissolved oxygen for stations in right-hand water in the eastern Gulf of Mexico, cruise 68-A-8.

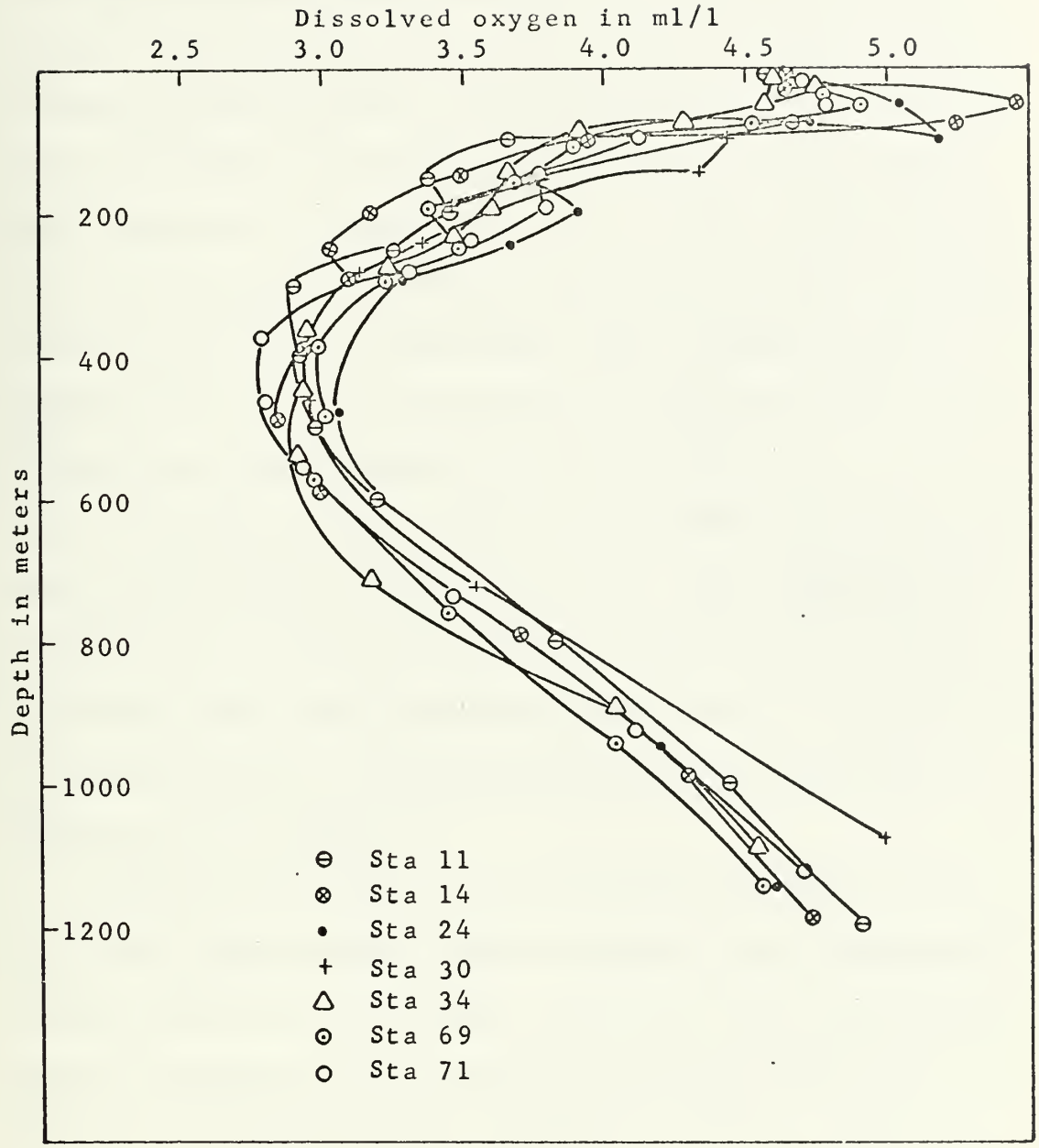

Figure 5
Vertical distribution of dissolved oxygen for stations in left-hand water in the eastern Gulf of Mexico, cruise 68-A-8.

near saturation. Supersaturated concentrations of 4.8 to 5.5 ml/l are found at the top of the thermocline at a depth of about 50 meters. The dissolved oxygen minimum of 2.8 to 3.0 ml/l is found between 400 and 600 meters in the left-hand water. This concentration is equivalent to 44 percent of saturation and agrees exactly with that found at the dissolved oxygen minimum in the right-hand water. No explanation is offered for the supersaturated concentrations at the top of the thermocline. While supersaturation is somewhat common in the upper 10 meters of the water column, it is unusual to be found at depths of 50 and 75 meters.

The dissolved oxygen minimum is much broader in the left-hand water and lies higher in the water column. Below 200 meters, the left-hand water appears to have the same characteristics as the right-hand water, but it has been displaced upward in the water column approximately 250 meters which reflects the adjustment of the mass to the circulation.

Seiwell (1938) points out the advantage of displaying some water mass characteristics, such as dissolved oxygen, independently of the depth scale. In this way, the picture is not distorted by vertical movements of the water mass as may be the case when characteristics are studied as a function of depth. It is now well established that the characteristics of the left-hand water in the Gulf of Mexico are found higher in the water column than the same characteristics in the right-hand water.

Seiwell (1938) plotted dissolved oxygen as a function of

salinity when studying its distribution in the Caribbean Sea. He found this relationship useful between the depths of 200 and 1200 meters in this area. Above 200 meters, phytoplanktonic growth and contact with the atmosphere may cause local variations. Below 1200 meters, the magnitude of salinity variation is too small for the relationship to be of any use.

Figures 6 and 7 are plots of dissolved oxygen versus salinity for right- and left-hand water respectively. Values for depths above 200 meters were not used for the reasons already mentioned. These two profiles appear very similar except near the top of Figure 7 (left-hand water) where the values begin to diverge due to the influence of the mixed layer. The shape of both curves is smoother for the left-hand water than for the right-hand water. This supports the theory that strong vertical mixing takes place in the left-hand water which was also seen in the temperature and salinity for this water.

The dissolved oxygen versus salinity curves found during cruise 68-A-8 are in close agreement with those determined from ATLANTIS I data taken in Yucatan Strait in 1933, 1934, and 1935 (Seiwell, 1938: figure 31A). The dissolved oxygen minimums found on cruise 68-A-8 range from 2.7 to 3.0 ml/l corresponding to a salinity of 34.9 to 35.1°/oo and a temperature of 8.5 to 9.5°C. These values are similar to those reported by Wust (1964) in the Caribbean.

Figure 6

Dissolved oxygen versus salinity for stations in right-hand water in the eastern Gulf of Mexico, cruise 68-A-8.

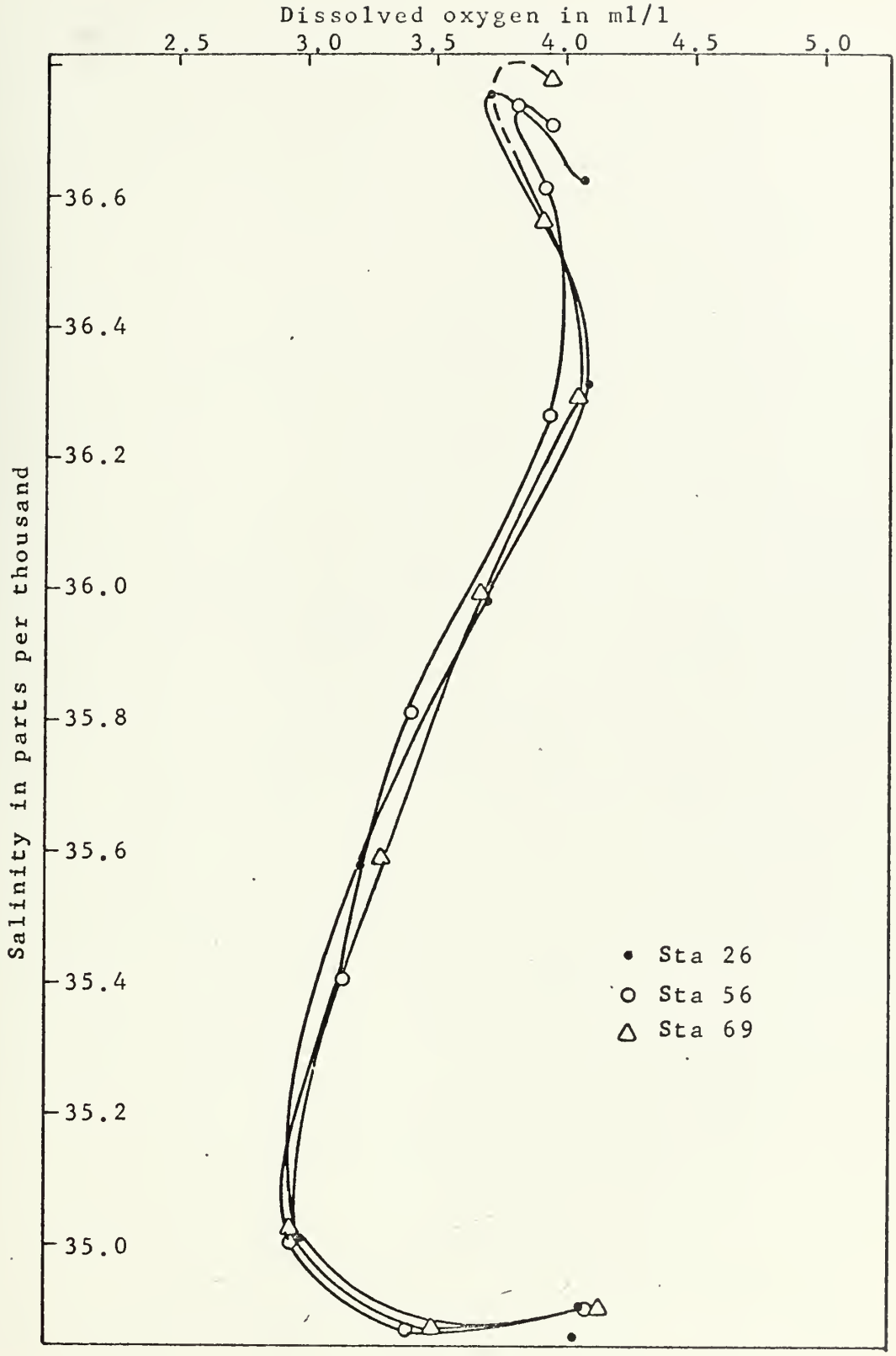
Dissolved oxygen in ml/l
2.5
3.0
3.5
4.0
4.5
5.0
Salinity in parts per thousand
36.6
36.4
36.2
36.0
35.8
35.6
35.4
35.2
35.0
Sta 26
Sta 56
Sta 69

Figure 7

Dissolved oxygen versus salinity for stations in left-hand water in the eastern Gulf of Mexico, cruise 68-A-8.

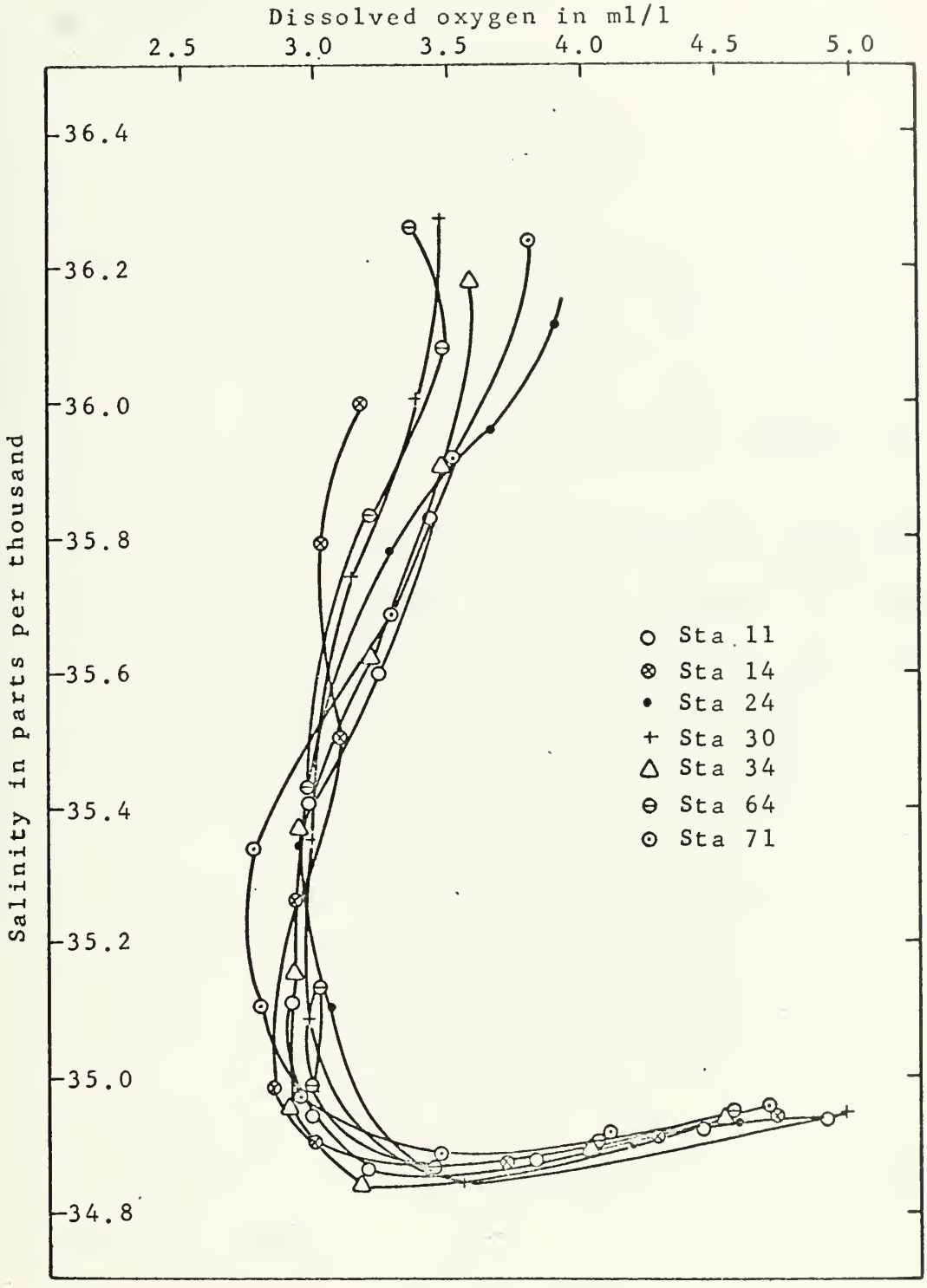
Dissolved oxygen in ml/l
2.5
3.0
3.5
4.0
4.5
5.0
Salinity in parts per thousand
36.4
36.2
36.0
35.8
35.6
35.4
35.2
35.0
34.8
Sta 11
Sta 14
Sta 24
Sta 30
Sta 34
Sta 64
Sta 71

CHAPTER IV

THE GULF LOOP

Salinity

The dynamic topography of the sea surface can be used to describe the loop current and is an acceptable definition of it. However, in this work, the current will first be described using the temperature and salinity distributions. The dynamic topography is discussed in Chapter V.

The water classified in Chapter III as mixed water (Figure 3) appears to be formed as a result of the lateral mixing of the right- and left-hand water. This occurs in the region of flow around the loop and as such, it can be an aid in locating and defining the loop. Mixed water is shown by the shaded portion of Figure 3. It forms a band about 30 nautical miles wide as it flows through the Gulf. The fact that the ship has entered the loop current is readily apparent by the angle of the hydrographic wire at stations, the set of the ship, and the topography of the isotherms. The loop extended into the Gulf about 350 nautical miles north of Yucatan Strait in August, 1968. Strong horizontal sheer must be present near station 39 due to the proximity of the north and south flowing portions of the current.

The description of currents and transport computations for this study are based on the assumption that the geostrophic

approximation will be representative of the conditions present. This requires that the Coriolis force and the pressure gradient force be the only ones acting and they must be in equilibrium. The field of mass is adjusted so that the less dense water is to the right of the direction of flow. In oceanic regions, the vertical salinity gradients are small and the slope of the isosteres is determined mainly by the vertical distribution of temperature. In this case, flow is assumed to be along the isotherms with the greater depths of the isotherms (warmer water) being to the right of the direction of the current. The strongest currents are found in the region where the isotherms have the greatest slope.

Figure 8 is a plot of surface salinity in the Gulf of Mexico. Surface salinities obtained at hydrographic stations and values of the hourly water samples have been plotted. The values during the first three days of the cruise were not plotted because this would have resulted in a considerable time variation (over two weeks) in some of the surface data in the same area of the western Gulf and in the vicinity of the Mississippi Delta. Surface salinities in the waters influenced by Mississippi River outflow may be subject to large variations over short periods of time. By eliminating the first short leg (less than three days in length) of the cruise, the data for the area west of the delta was spread over two days and is, therefore, more synoptic.

The horizontal distribution of surface salinity gives a fair indication of the circulation of the loop current. The current is

Figure 8

Surface salinity in parts per thousand, cruise 68-A-8. Contour interval 0.2^{o}/oo above 36.0^{o}/oo (dashed lines) and 0.5^{o}/oo below 36.0^{o}/oo (solid lines). Open circles indicate the axis of the maximum surface salinity, closed circles indicate the axis of the minimum surface salinity. Data from 329 surface salinity samples.

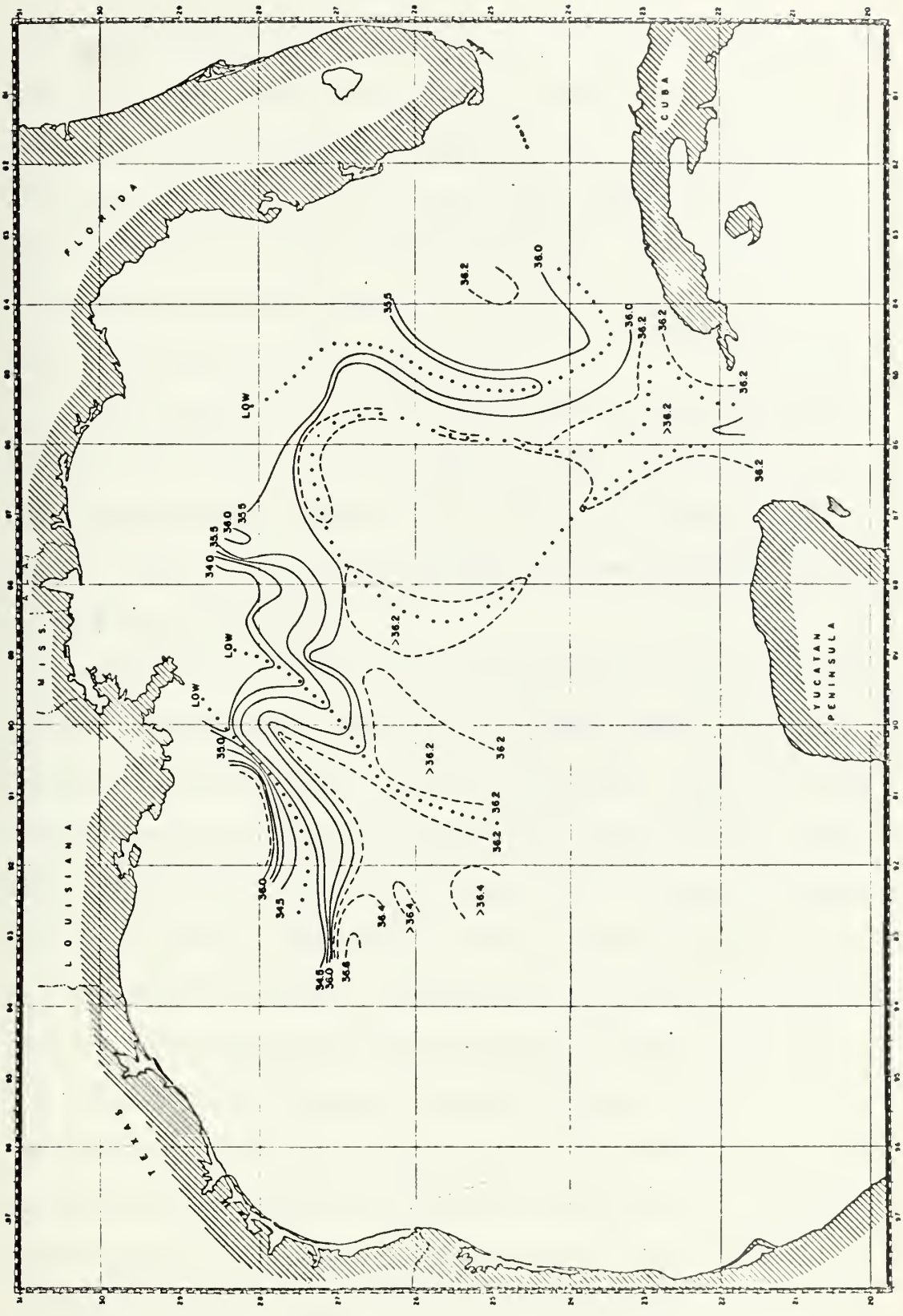
FLORIDA
CUBA
YUCATAN PENINSULA
LOUISIANA
TEXAS
MISS.
LOW
LOW
LOW
34.0
34.5
35.0
35.5
36.0
36.2
>36.2
36.4
>36.4

generally enclosed by the 36.2°/oo isohaline at the surface and the approximate core shows up as a ridge of high salinity indicated by the open circles in Figure 8. The horizontal distribution of salinity at 100, 150, and 200 meters (not shown) reveals the presence of the loop circulation more clearly. These plots also support the circulation features indicated by the tongues of low surface salinity to be discussed next.

Three tongues of low surface salinity are evident and are indicated by solid circles in Figure 8. At least two of these tongues appear to originate in the vicinity of the Mississippi Delta. The three low salinity tongues indicate additional surface circulation in the Gulf.

One tongue is first seen at the northeast corner of the loop current and generally parallels the southward flowing portion of the current. It is found near stations 19, 63, 60, 47, and 41. This tongue has values of surface salinity less than 35.50°/oo. The Atlas of Pilot Charts, Central American Waters and South Atlantic Ocean (H. O. Pub. No. 106) shows a wide southern flow just off the Florida Shelf that probably includes both the stronger loop current and the flow indicated by this low salinity tongue to the east of it.

The Atlas also depicts a northward flowing surface current off the west coast of Florida. This current is probably fed, at least in part, by this tongue of low surface salinity east of the loop current that flows southward, curves around to the left in the area of BT 157, and then flows northward toward Florida. The circulation

in this region can not be completely described because cruise 68-A-8 did not extend far enough to the east in this area.

A second tongue of low salinity extends westward at the surface from the area of the Mississippi Delta passing near station 77 and 80 and then up on the continental shelf off Texas. The surface salinity values here are less than $34.50^{o}/oo$. This flow is consistent with the surface currents shown in the Pilot Charts for this time of year.

The third flow is perhaps the most interesting. The contours of surface salinity indicate a current flowing to the southwest from the region of the Mississippi Delta. This tongue of low salinity passes near stations 75, 8, and 86. The Pilot Charts do not show a southwesterly surface current in this area but indicate a more westerly drift. This is possibly the result of the prevailing easterly and southeasterly winds having a greater effect on ship drift in this area than this relatively narrow current. This southwesterly flow is in agreement with drift bottle studies of surface currents in 1961 and 1962 by Drennan (1963). He has reported that drift bottles released near the delta have been recovered along the Mexican coast as far south as Coatzacoalcas (18°-09'N, 94°-25'W), indicating a flow that continues to the southwestern part of the Gulf. He found this southwest flow at speeds of 0.50 m/sec (1.0 knot) or more from August to October in both 1961 and 1962. These flows are supported by the dynamic topography of the sea surface relative to the 1000 decibar surface

to be discussed in Chapter V.

The depth of the subsurface salinity maximum is shown in Figure 9. At Yucatan Strait the salinity maximum enters the Gulf of Mexico at depths of 150 to 200 meters. The salinity maximum in this layer, 36.73°/oo, is confined to the right-hand water in the eastern Gulf. The depth of this layer in the right-hand water is consistent with the depth of this feature in the Caribbean (Wust, 1964).

Vertical Cross Sections

Figures 10, 11, and 12 show the vertical cross sections of temperature, salinity, and thermosteric anomaly respectively at transect one in Yucatan Strait. See Figure 1 for the location of the transects. Transect one includes stations 31 through 35. The temperature cross section, Figure 10, shows the increased slope of the isotherms west (left) of station 33 and the strong vertical temperature gradients in the surface layers. The additional data points between stations in this figure are from BT data.

The salinity cross section is similar in that it shows the greater slopes west of station 33. It also shows clearly the remnant of the Subtropical Underwater with its high salinity core entering the Gulf at a depth of 150 to 200 meters near the center of the cross section. The salinity maximum has a value of 36.73°/oo at station 32. The remnant of the Subantarctic Intermediate Water appears as a salinity minimum and is indicated by the dashed line

Figure 9

Depth to the core of the salinity maximum, cruise 68-A-8. Depth in meters, contour interval 25 meters.

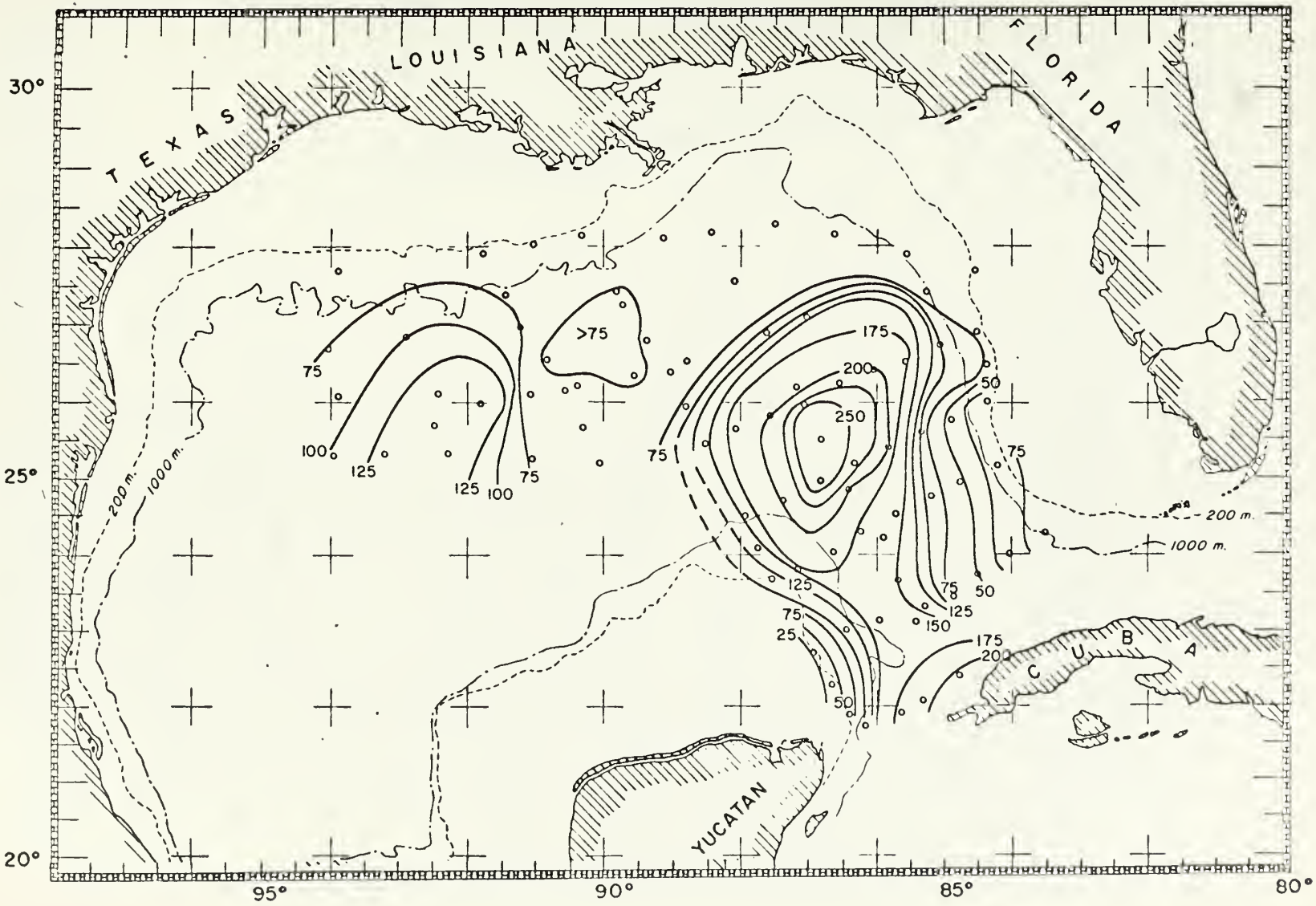
LOUISIANA
TEXAS
FLORIDA
30°
25°
20°
95°
90°
85°
80°
>75
75
100
125
125
100
75
175
200
250
50
75
75
125
75
50
125
150
75
25
50
175
200
200 m.
1000 m.
200 m.
1000 m.
C U B A
YUCATAN

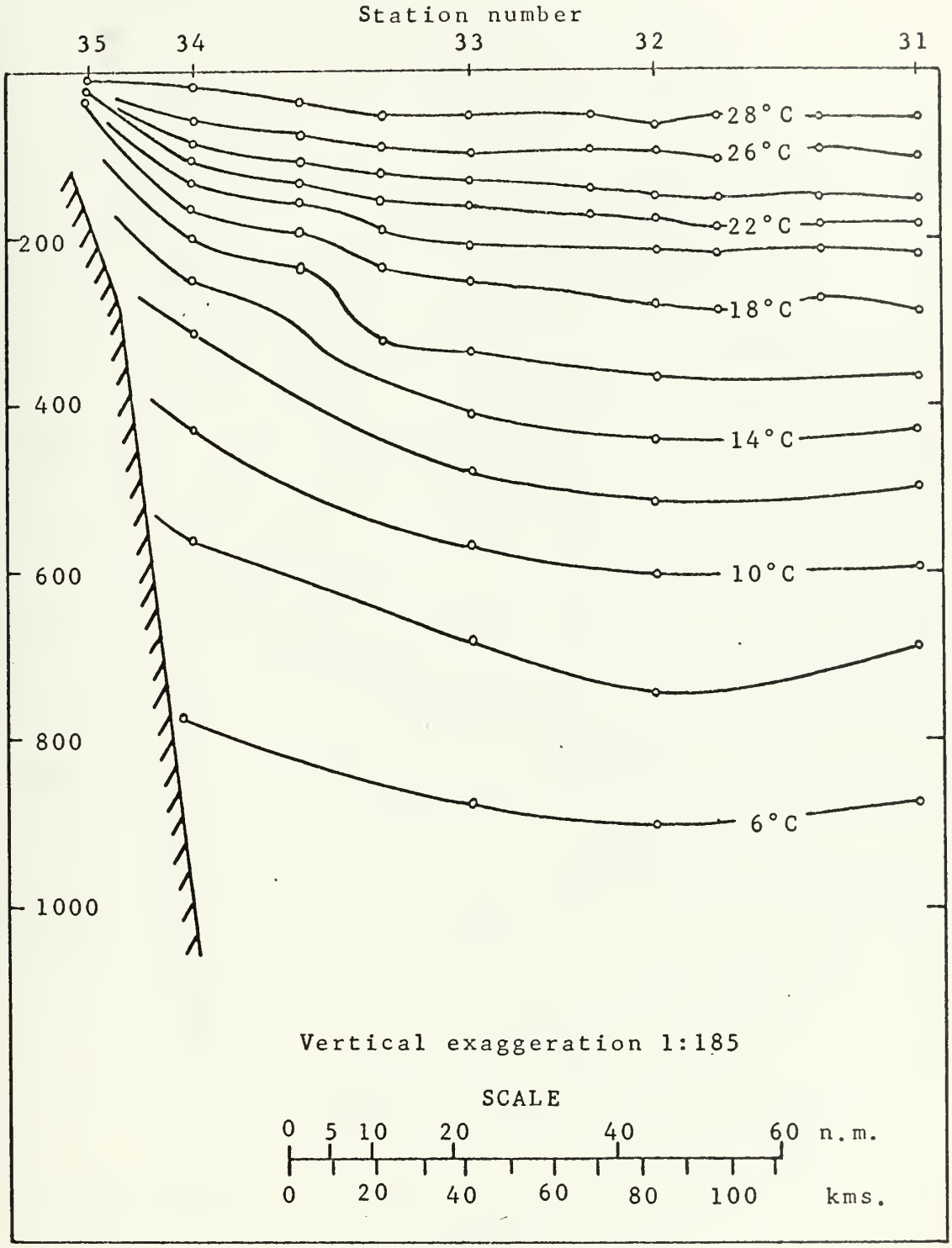

Figure 10
Temperature/depth profile across Yucatan Strait. Depth in meters, temperature in degrees Centigrade.

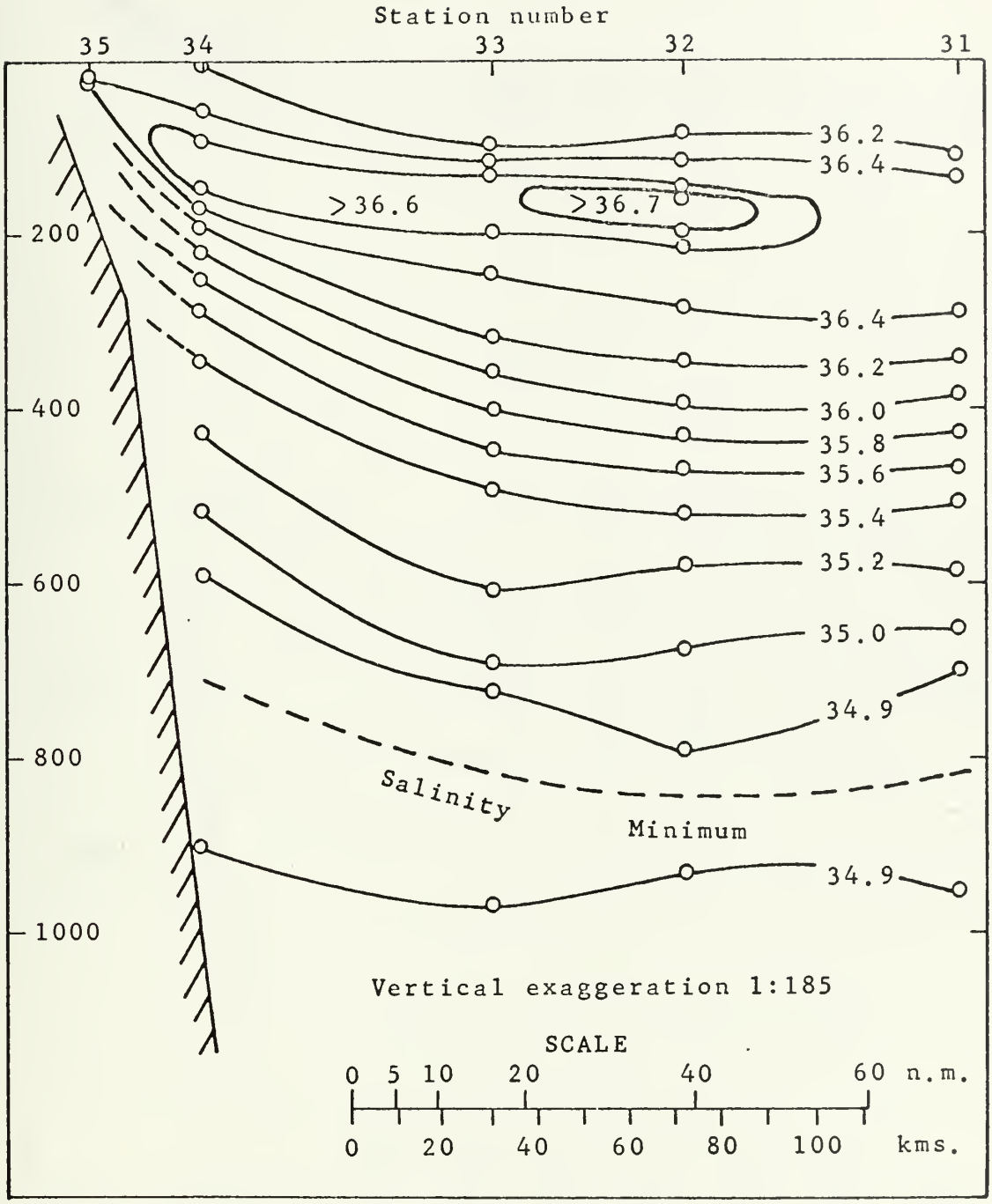

Figure 11

Salinity/depth profile in Yucatan Strait. Depth in meters, salinity in parts per thousand.

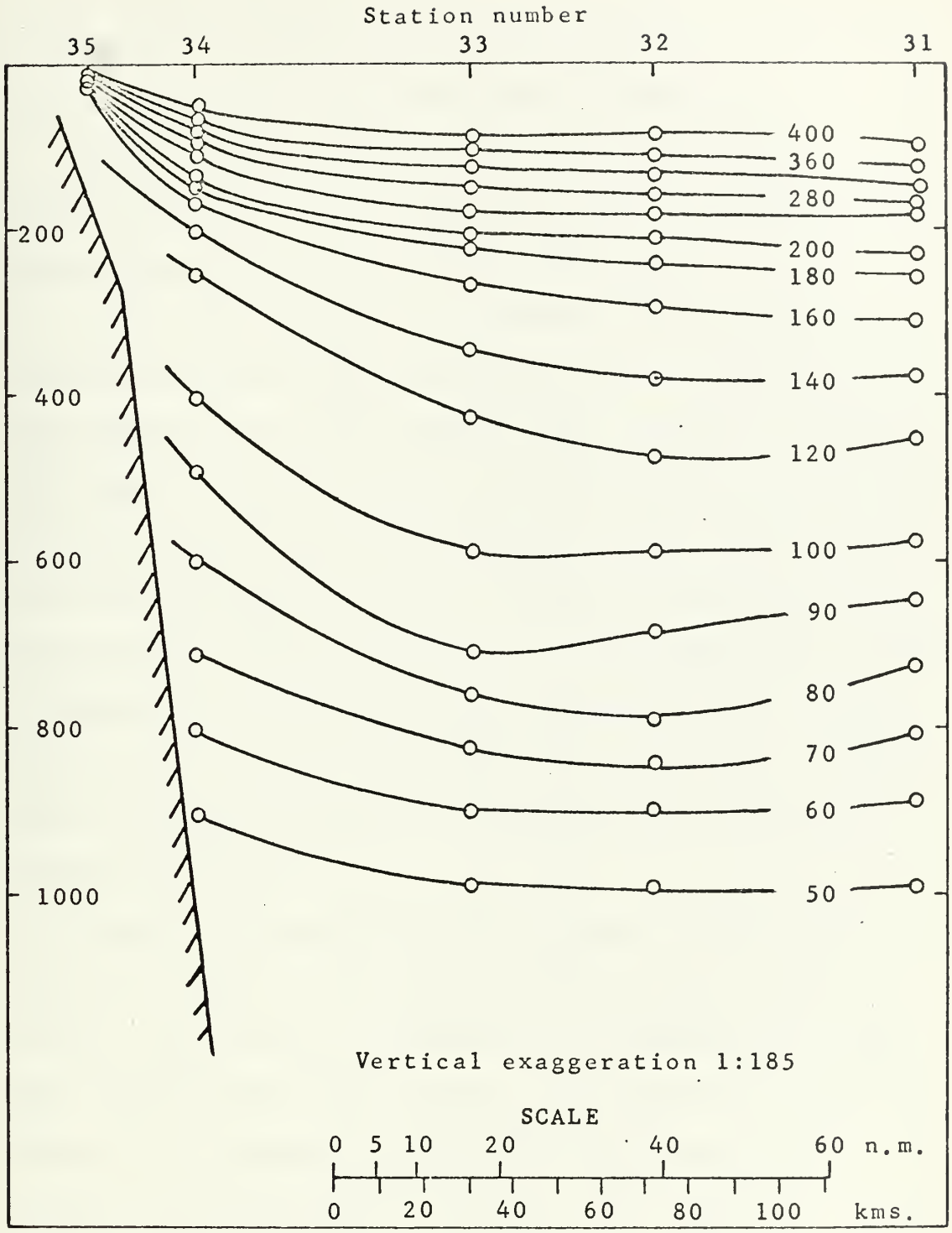

Figure 12

Thermosteric anomaly/depth profile across Yucatan Strait. Depth in meters, thermosteric anomaly in centiliters per metric ton.

in Figure 11. The value of the salinity minimum is 34.85°/oo in Yucatan Strait and is found near a depth of 800 meters.

Figure 12 depicts the isosteres in this cross section. The isosteres also have greater slopes west of station 33 which reflect the adjustment of the field of mass to the flow.

It has been found that the topography of the selected isotherms in the upper 300 meters gives a very good indication of the location of the current (Leipper, 1967). Temperature data in this region of the water column is readily obtained from BTs. When interpreting the isothermal topography, the flow is assumed to be along the isotherms with the greater depth of the isotherm (warmer water) lying to the right of the current. The speed of the current is proportional to the slope of the isotherms although no attempt is made here to estimate the current speed in this manner. Therefore, a relatively complete picture of the loop current can be obtained from BT data.

Figures 13 through 18 show the topography of selected isotherms in the upper 275 meters on six transects across the loop current. The transects in these figures are numbered two through seven proceeding from south to north. The locations are shown in Figure 1. The transects are oriented 070-250 degrees (except transect seven) and average 220 nautical miles in length.

Transect two crosses the neck of the loop current and shows a northward (into the paper) flow near BT 145 and the southward flow near BT 150. There is an indication of a weak flow to the south

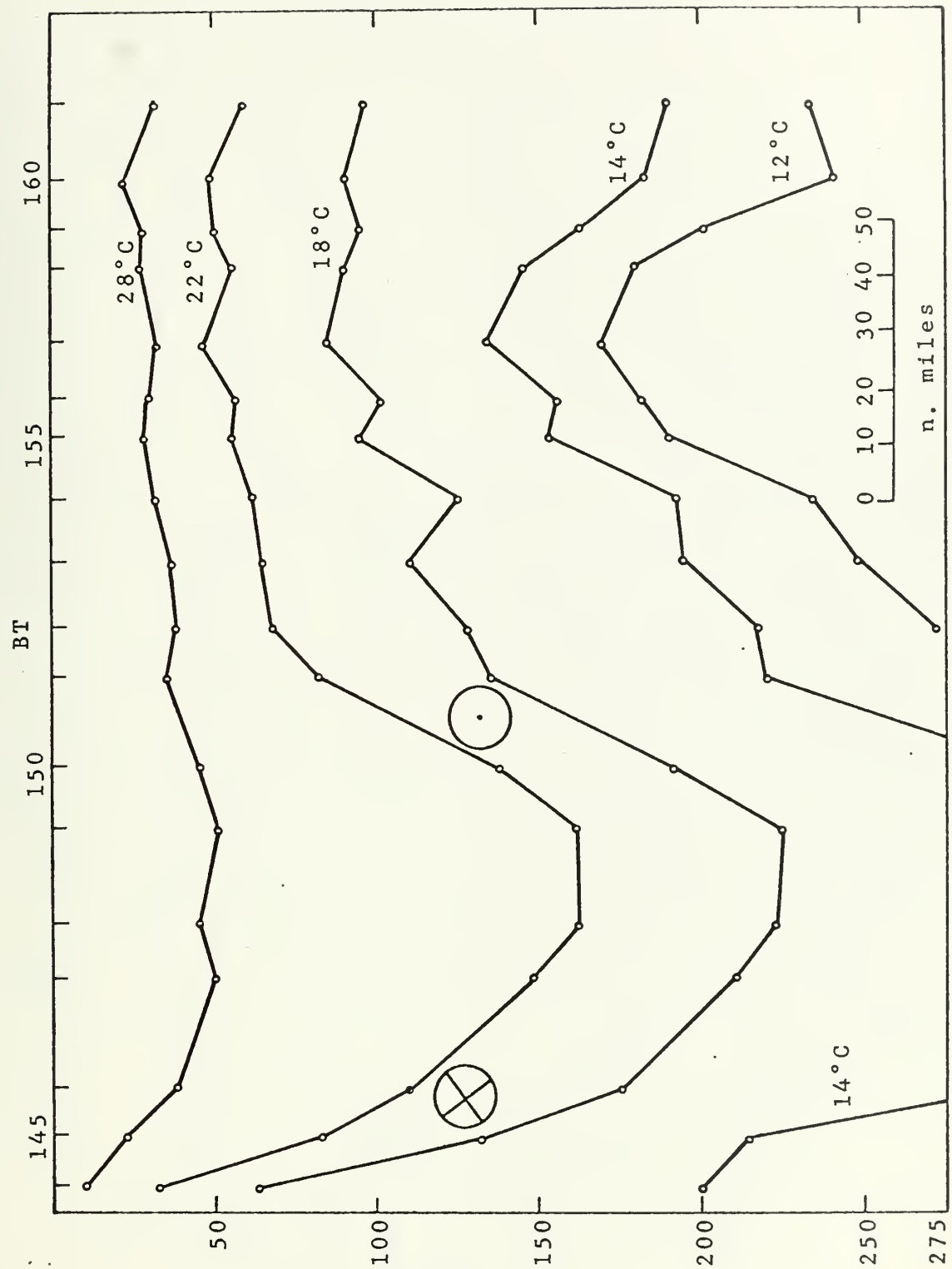

Figure 13

Depth of isotherms at transect two. Depth in meters, temperature in °C, vertical exaggeration 1:1100.

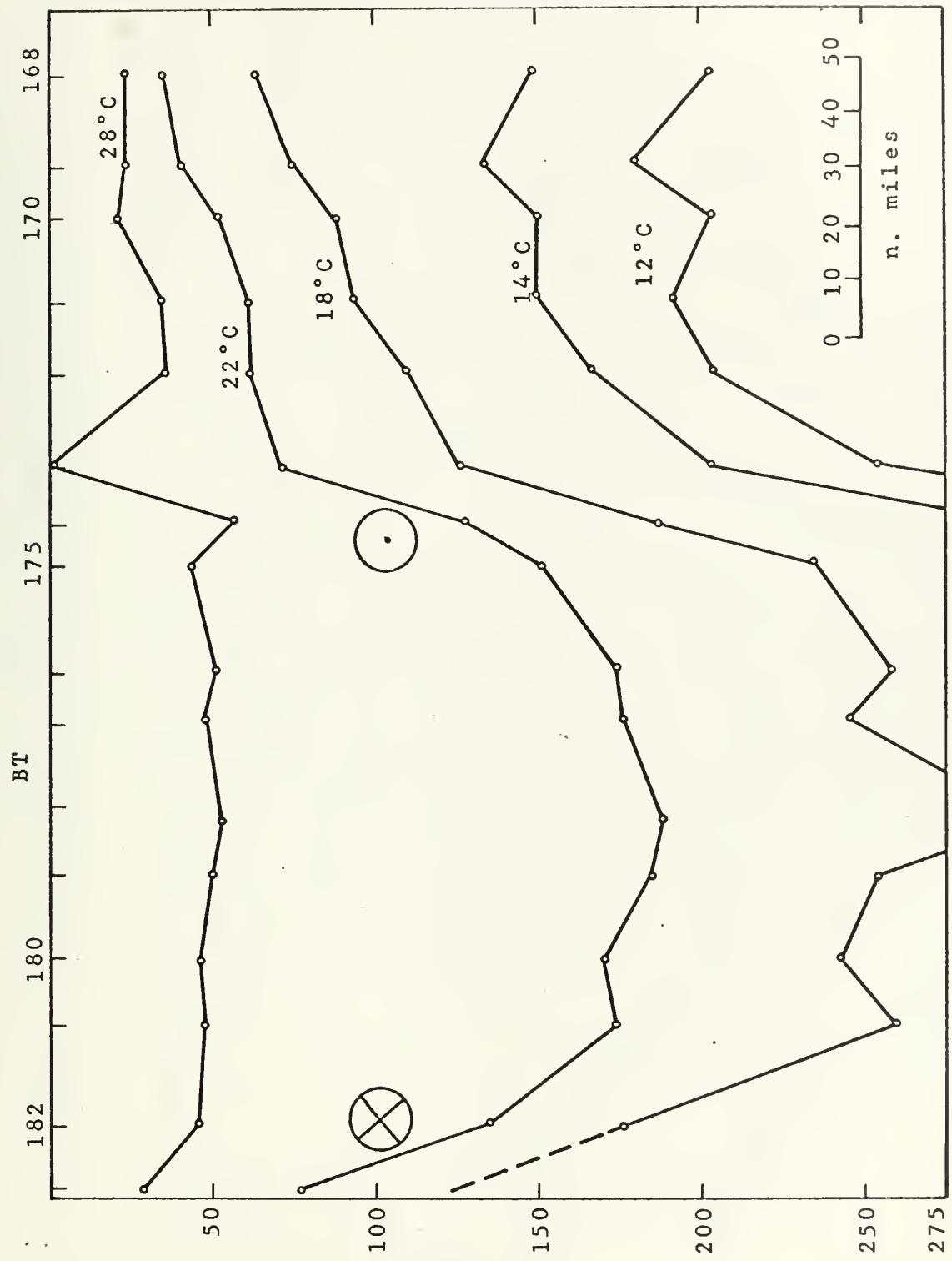

Figure 14
Depth of isotherms at transect three. Depth in meters, temperature in °C, vertical exaggeration 1:1100.

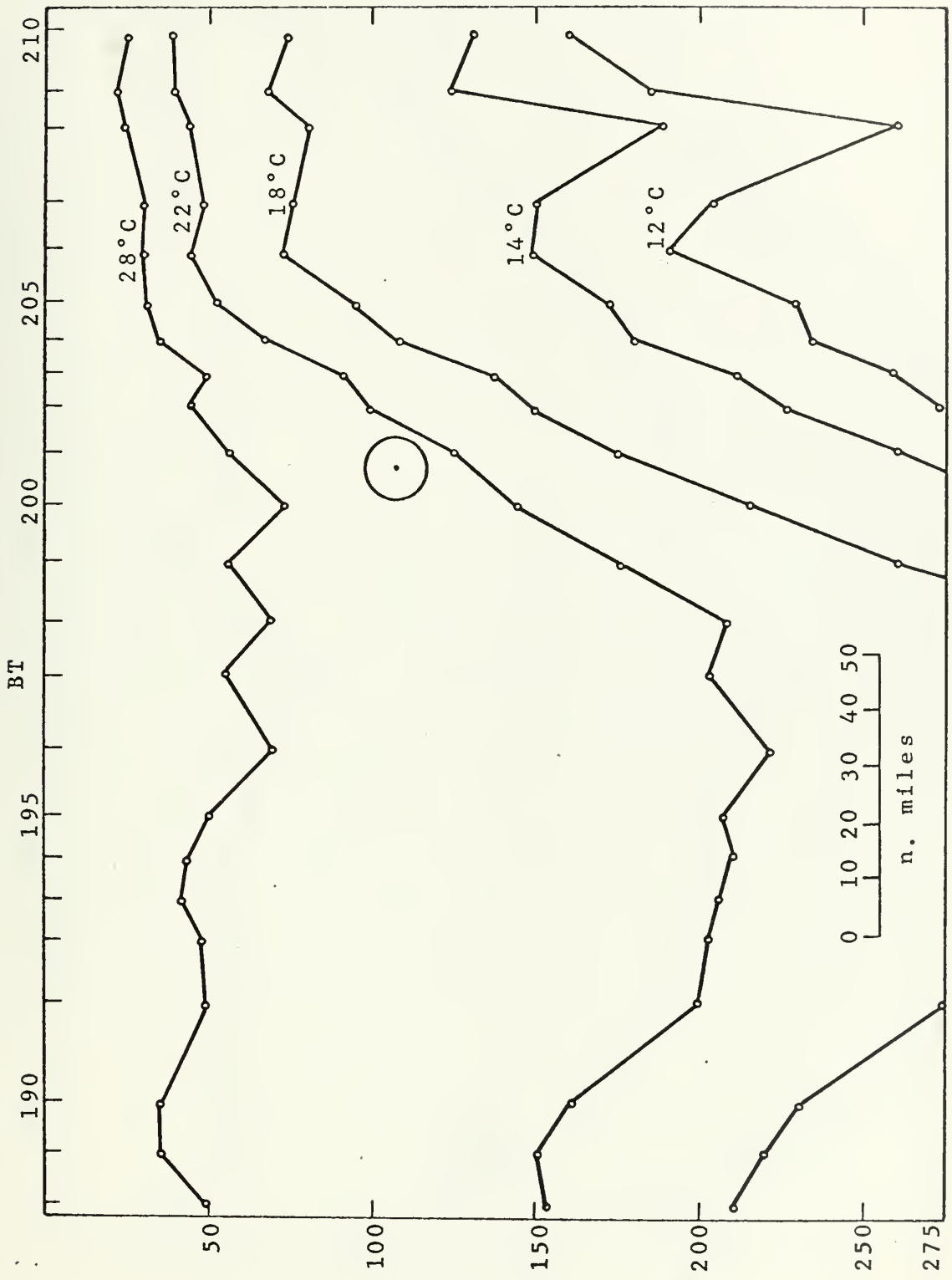

Figure 15
Depth of isotherms at transect four. Depth in meters, temperature in °C, vertical exaggeration 1:1100.

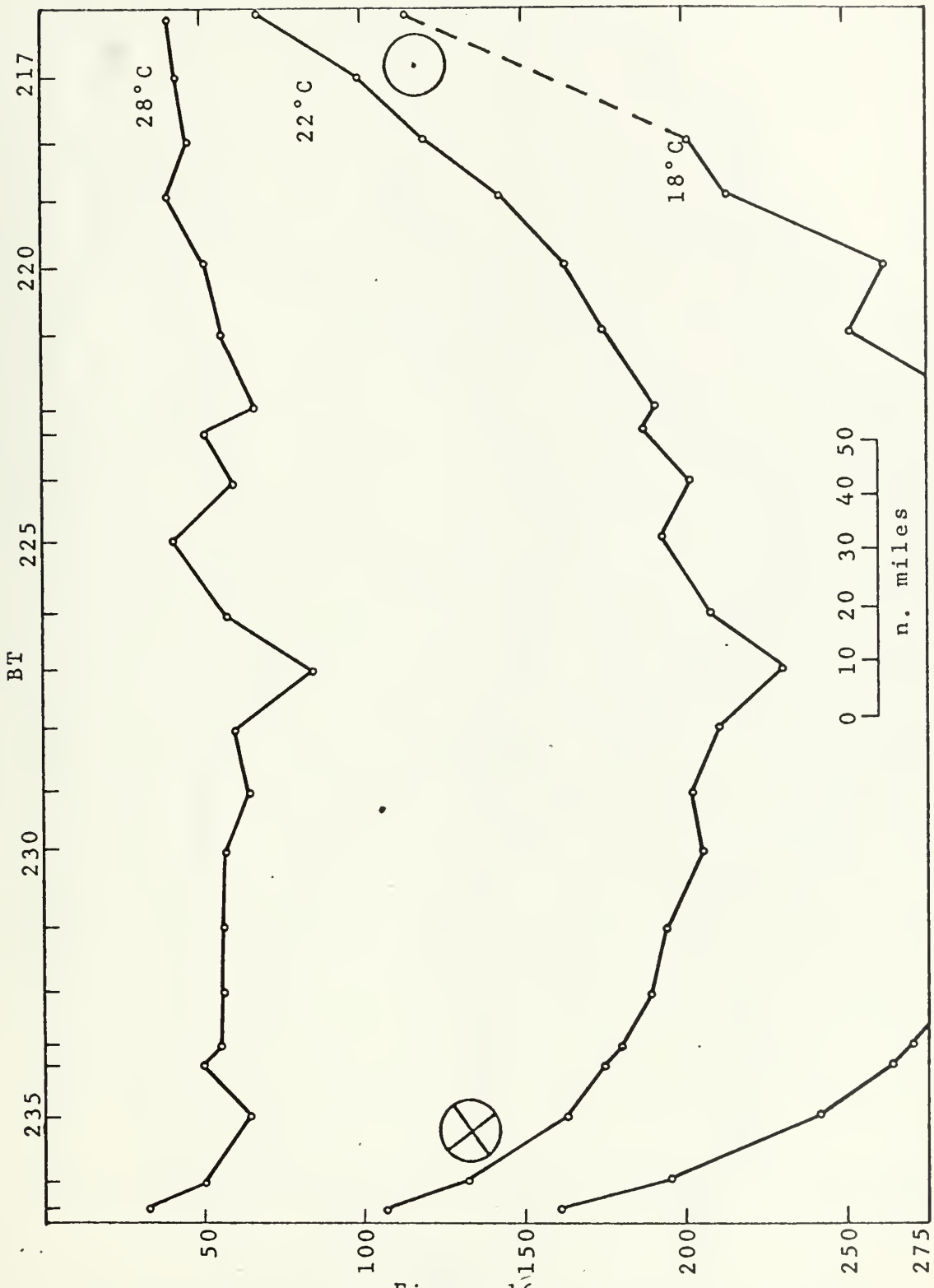

Figure 16

Depth of isotherms at transect five. Depth in meters, temperature in °C, vertical exaggeration 1:1100.

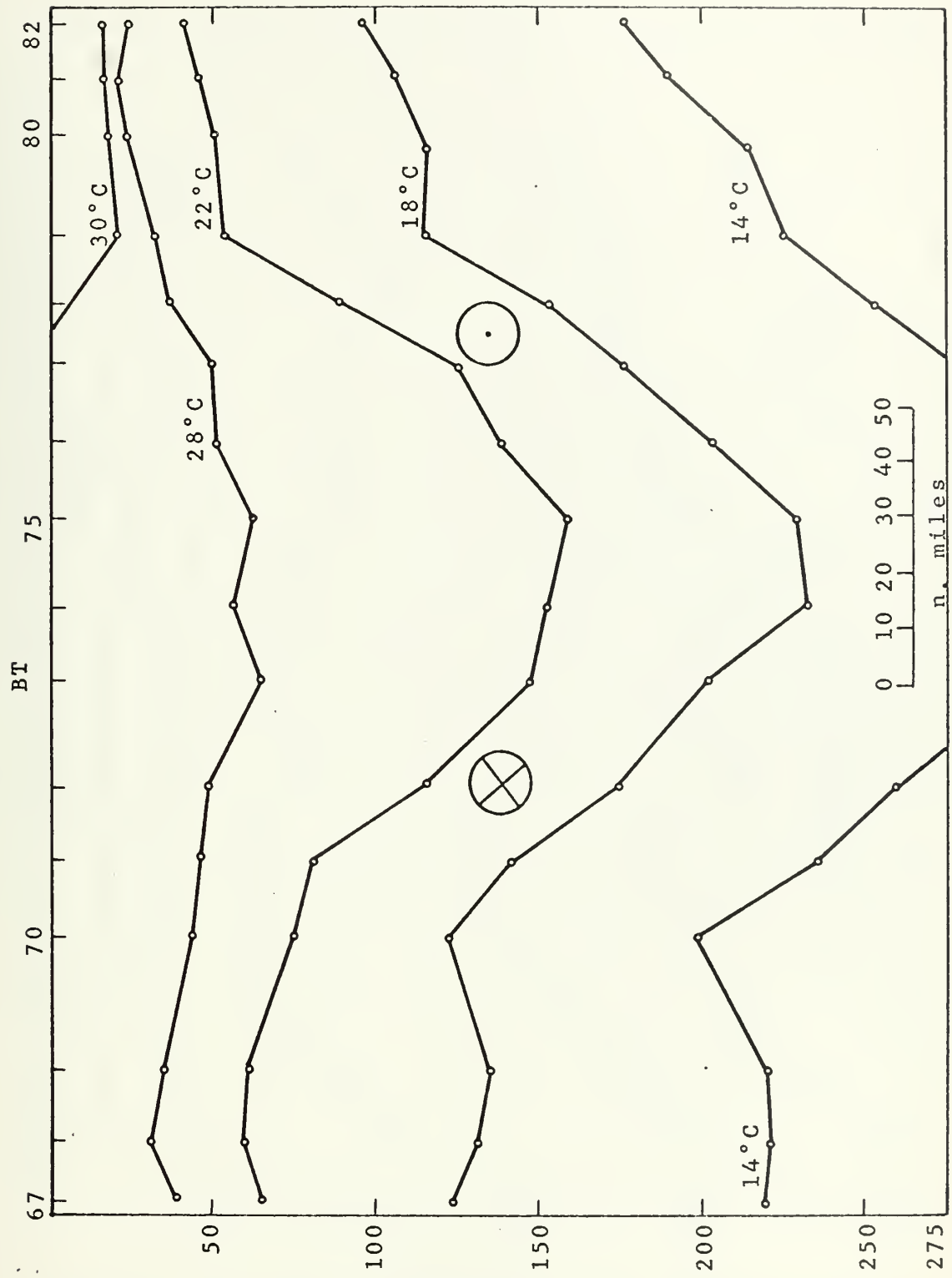

Figure 17
Depth of isotherms at transect six. Depth in meters, temperature in °C, vertical exaggeration 1:1100.

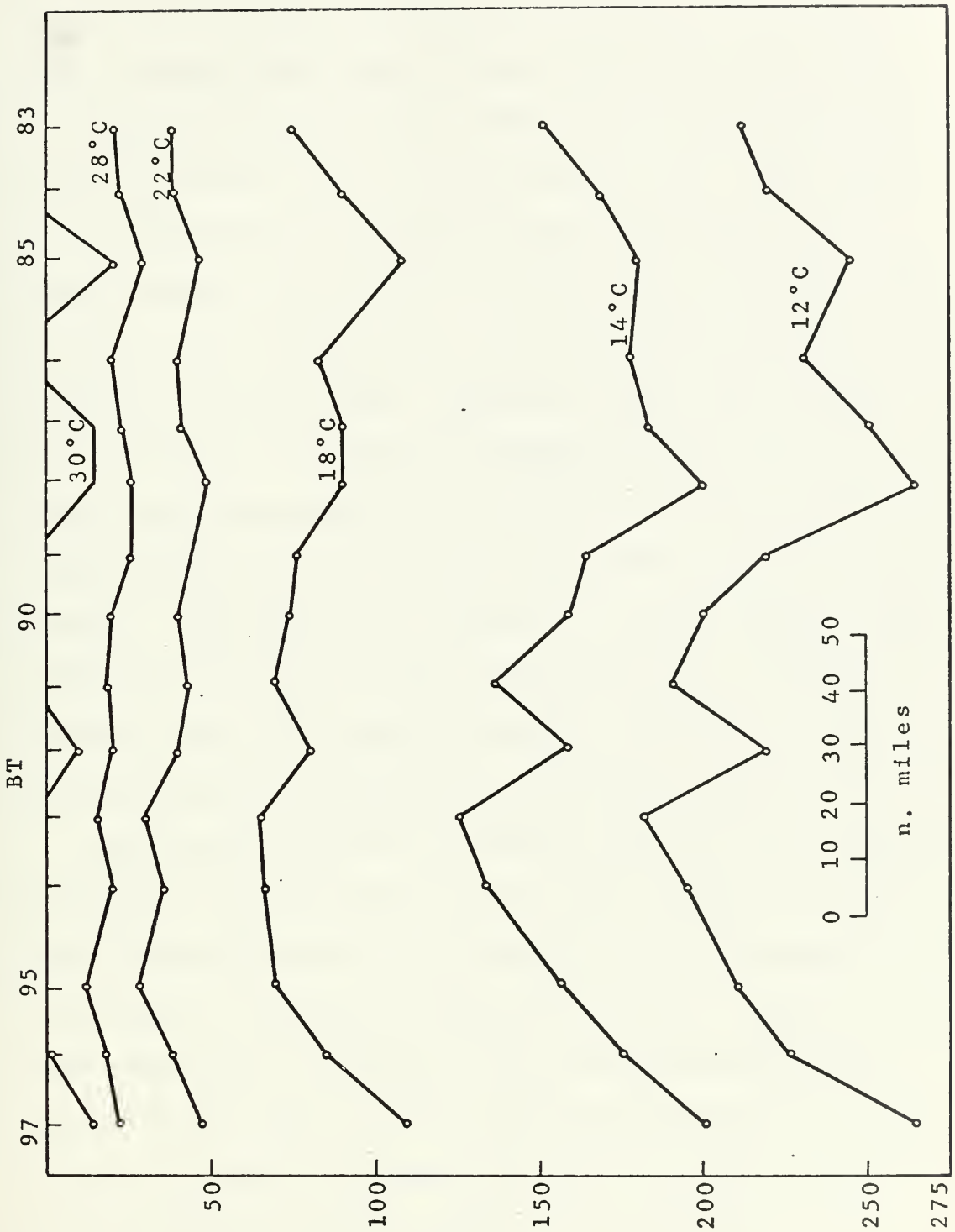

Figure 18
Depth of isotherms at transect seven. Depth in meters, temperature in °C, vertical exaggeration 1:1100.

circling around BT 157 and flowing north again toward the Florida Shelf. Transect three shows a strong northward flow near BT 182 and southward flow near BT 174. This transect did not extend far enough to the west to cross all the northern flow. There appears to be another smaller southward flow near BT 199 and BT 206. A lesser southerly flow is indicated in the vicinity of BT 209. The main part of the northward flow is west of BT 188 and was not covered by the cruise track. Transect five shows the northward flow centered at BT 235 and the southward flow near BT 217. At transect six, the northern portion of the loop is seen extending between BT 70 and BT 79. The flow here is nearly parallel to the transect. The slopes of the isotherms at transect seven show some evidence of a current, but other data indicate it is not part of the loop current. The slope of isotherms near BT 97 indicates a southward flow and is probably due to Mississippi River outflow.

These figures describe the thermal structure at the transects and indicate the flow there, but it is still difficult to see the areal pattern of the flow. To overcome this, it is customary to use the horizontal topography of isothermal surfaces. Comparison with other cruises can be simplified if the same isothermal surface is used. Leipper (1967) has found that the 22°C isotherm can be used all year to indicate the position of the loop current. The depth of this isotherm is shown in Figure 19. The strongest flow, as indicated by the slope of the isotherms shown at the transects (Figures 13 through 18), corresponds to a depth of the 22°C isotherm

Figure 19

Depth of the 22°C isotherm, cruise 68-A-8. (After Leipper, 1968e).

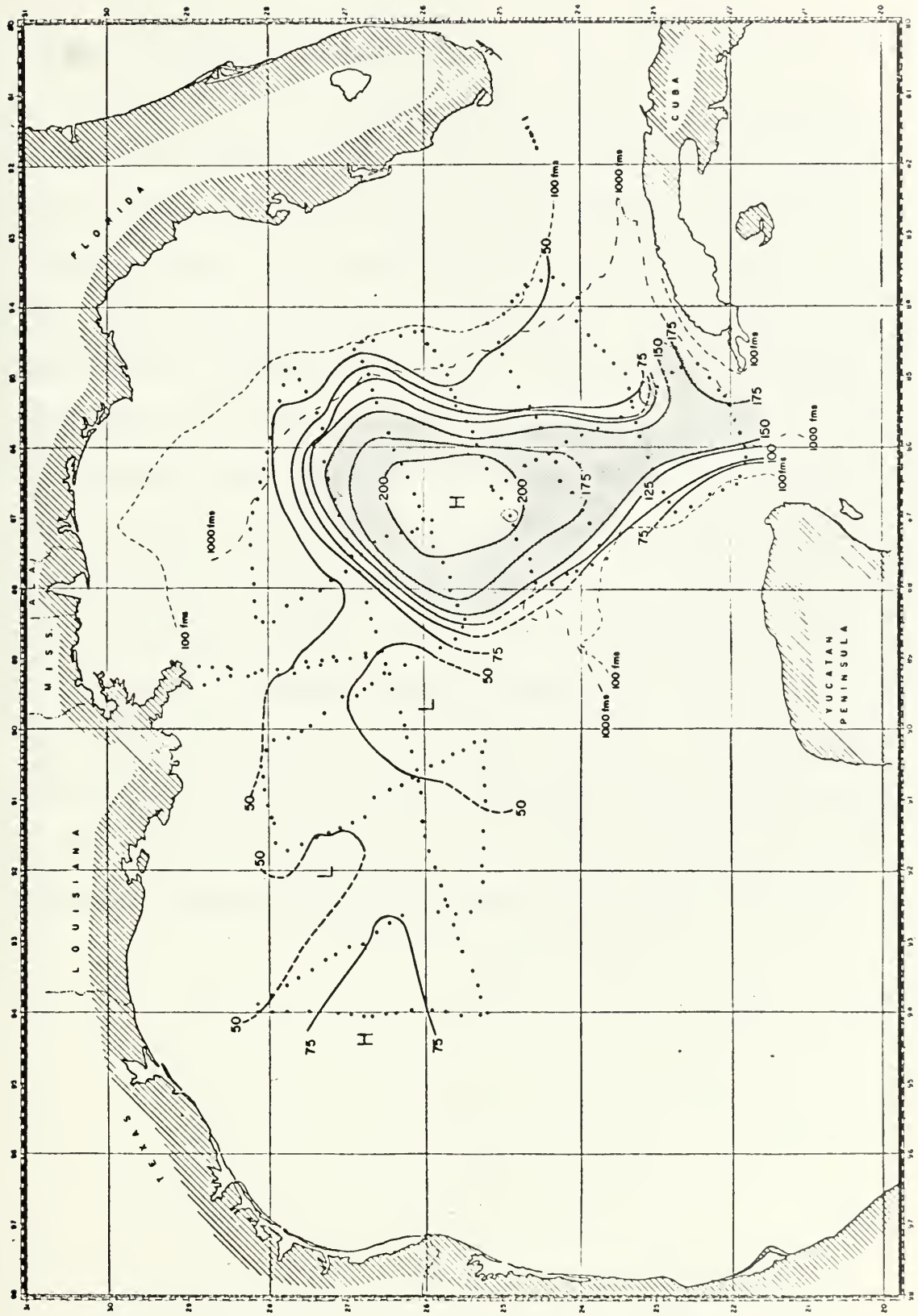
FLORIDA
CUBA
MISSISSIPPI
LOUISIANA
TEXAS
YUCATAN PENINSULA
100 fms
1000 fms
H
L
50
75
100
125
150
175
200

of 125 to 150 meters (Figure 19).

Cochrane (1966) has mentioned the occurrence in some years of a small but distinct patch of cool surface water near the current core. The drop in surface temperature ranged from 0.5 to 2.0°C below the values of the surrounding water. He attributes this to upwelling representing a line of divergence. A similar feature was observed in August, 1968. After BT 138, the intake temperature dropped 0.7°C and then rose again in a period of 10 minutes. This was observed on the shipboard infrared thermometer recorder also. This feature was about 4 kilometers wide and was located west of the current core similar to those reported by Cochrane except this one was somewhat narrower. The water depth was 200 meters. The feature was not recrossed when heading eastward on the next transect and probably went unnoticed as the ship crossed it on the leg from station 35 to 37. On this leg, the feature would be almost parallel to the ship's track and the change would have been very gradual. Additional temperature distributions are discussed in Chapter VI.

CHAPTER V

CURRENTS AND TRANSPORT

The computation of relative volume transport in the loop current is based on the assumption that this circulation satisfies the geostrophic approximation. This requires that the Coriolis force and the pressure gradient force be the only two forces acting and that they be in equilibrium. The method in Defant (1961: page 494) was used at first to determine the topography of the reference level. Graphs showing the difference in dynamic heights versus depth (not shown) indicated that the reference level was below 1000 decibars. Hubertz (1967), using the same procedure, found this level to be 1350 decibars during June, 1966, in the eastern Gulf of Mexico. However, his transport values show that less than 1 million m^3/sec, or less than two percent of the total transport, occurs between the 1050 and 1350 decibar surfaces. Based on this fact and in order to make use of the greatest possible number of stations, the 1000 decibar surface was selected as the reference level for this work. Small errors in transport may result from the selection of this level.

Figure 20 depicts the dynamic topography of the sea surface (in dynamic meters) relative to the 1000 decibar surface. A high of 1.99 dynamic meters was found at station 26. A lesser high of 1.74 dynamic meters was located near stations 31 and 32, just north of the western end of Cuba. A ridge, whose crest is indicated

Figure 20

Dynamic topography of the sea surface relative to the 1000 decibar surface, cruise 68-A-8. Contour interval 0.1 dynamic meters, crossed dashed line indicates the crest of the dynamic ridge.

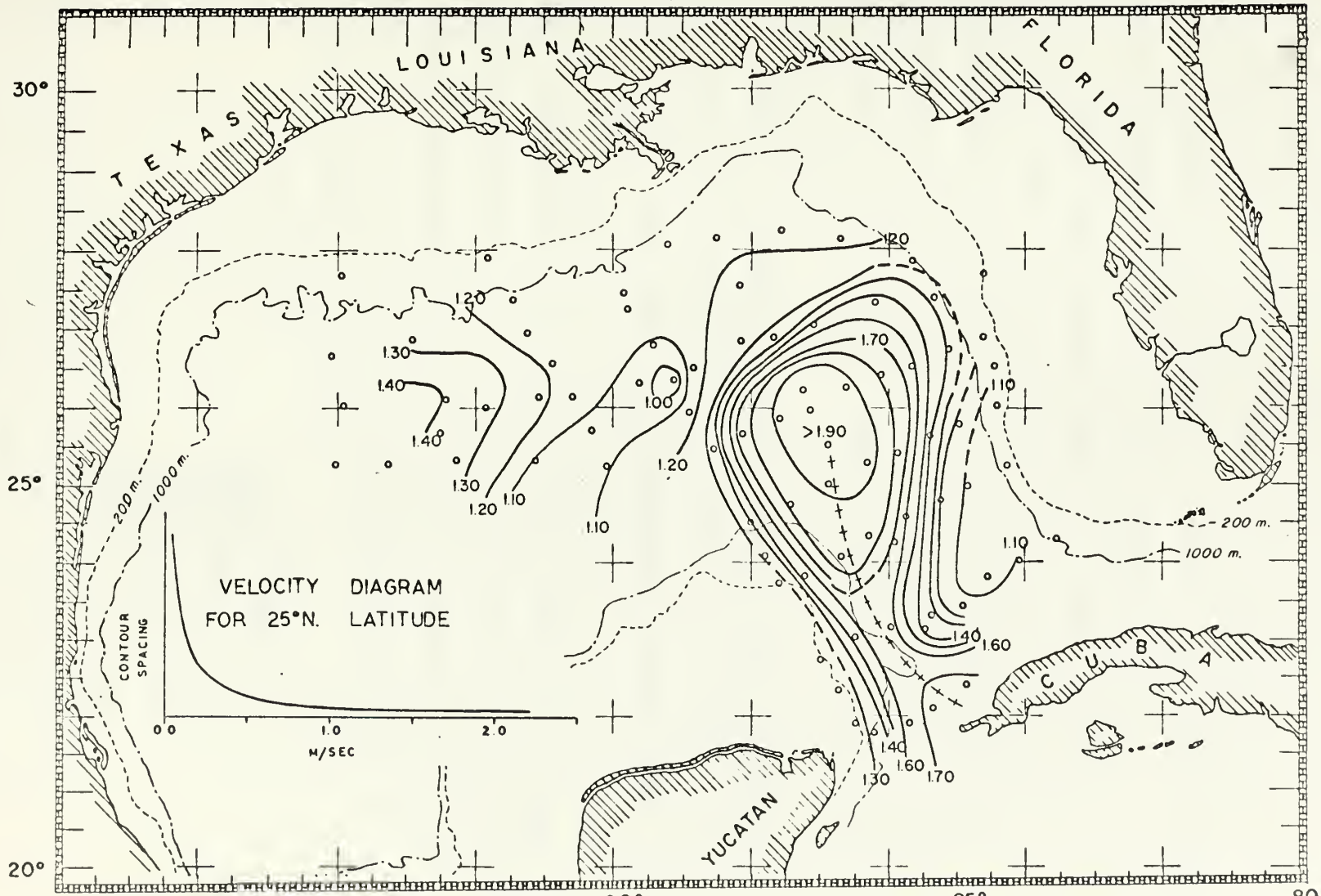
LOUISIANA
TEXAS
FLORIDA
CUBA
YUCATAN
30°
25°
20°
95°
90°
85°
80°
200 m.
1000 m.
1.20
1.30
1.40
1.10
1.00
1.70
>1.90
1.60
VELOCITY DIAGRAM
FOR 25°N. LATITUDE
CONTOUR SPACING
0.0
1.0
2.0
M/SEC

by the crossed dashed line, extends from station 26 southward near stations 56, 50, and 39 toward Cuba. The dynamic topography is nearly symmetric about this ridge. The value of the surface currents can be obtained by making use of the velocity diagram.

The geostrophic transport field for the upper 1000 meters relative to 1000 decibars is shown in Figure 21. The vertical integration of the dynamic height relative to 1000 decibars was carried out using the equation in McLellan (1965: page 71). The Coriolis factor was calculated using the middle latitude between each station pair.

Based on the dynamic topography, station 26 was considered to be at the center of the anticyclonic eddy and the transport value there is zero. The value of the streamlines increases outward from station 26 in intervals of 10 million m^3/sec. At Yucatan Strait, 46.7 million m^3/sec of water flow northward into the Gulf between stations 31 and 34. In three sections extending across the current radially from station 26 (see Figure 21 for location), transports greater than 50 million m^3/sec were found in August, 1968. In tabular form these transports are:

Station pair	Transport
26-71	53.8 million m^3/sec
26-24	52.5 million m^3/sec
26-64	50.9 million m^3/sec

These figures indicate a fairly uniform transport around the northern portion of the loop. Hubertz (1967) reported similar

Figure 21

Streamlines of geostrophic transport in the upper 1000 meters relative to 1000 decibar surface, cruise 68-A-8. Contour interval 10 million m^3/sec.

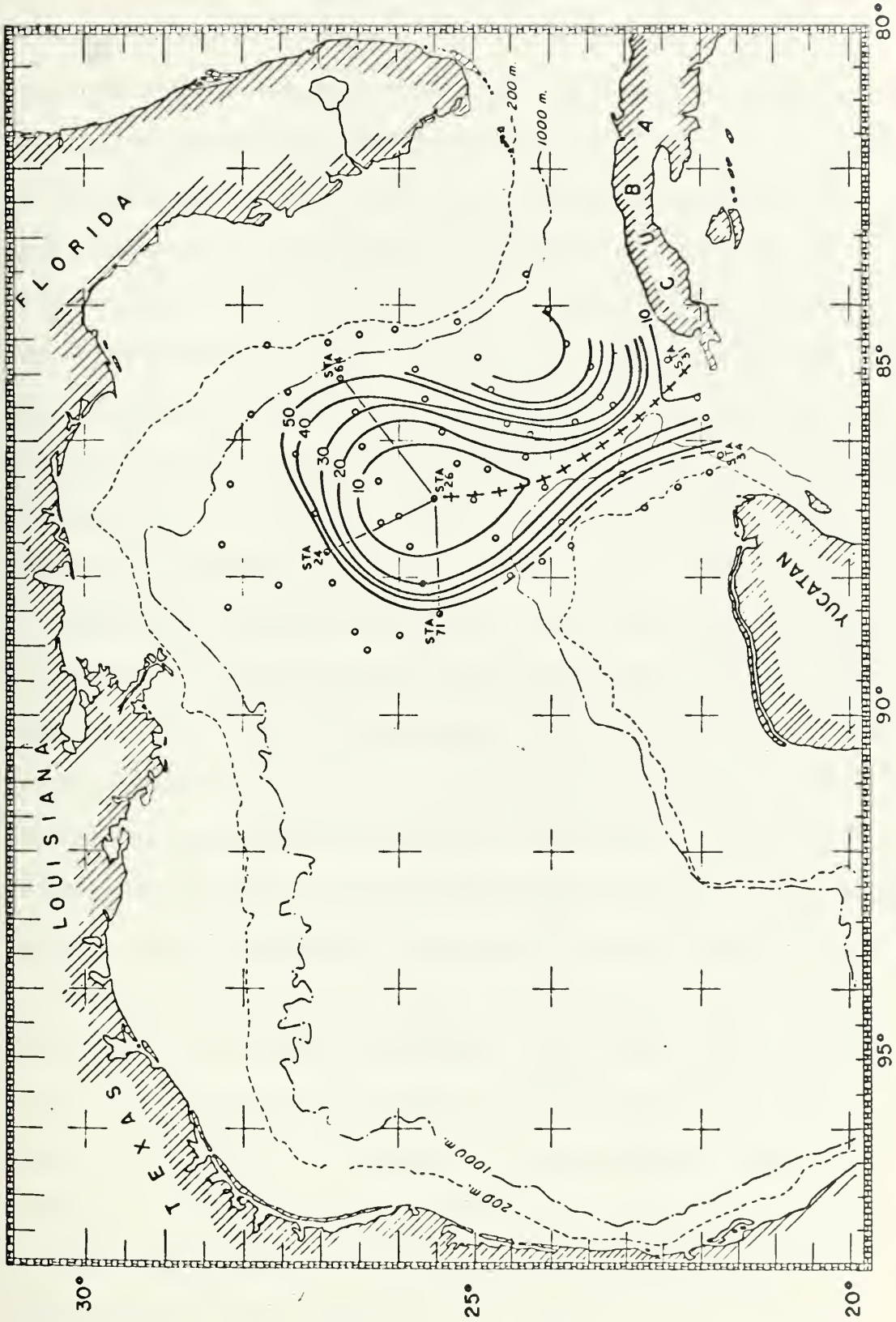
FLORIDA
LOUISIANA
TEXAS
YUCATAN
200 m.
1000 m.
200 m
1000 m
A
B
C
10
20
30
40
50
STA 64
STA 26
STA 24
STA 71
STA 53
STA 34
80°
85°
90°
95°
30°
25°
20°

values of transport for this part of the loop in June, 1966. The transects calculated during August, 1968, are among the highest ever reported for Yucatan Strait and the loop current.

The section across the path of the outflow toward Florida Straits (stations 30 to 31) has a transport to the east of 37.7 million m^3/sec. This is in reasonable agreement with the steady state volume transport of 32 ± 3 million m^3/sec measured in the Florida Current by Schmitz and Richardson (1968). Their figure is the result of direct current measurements equivalent to more than 50 transects across the current over a period of three years. Monthly averages were found to fall within this range.

The values of geostrophic transport entering the Gulf through Yucatan Strait (stations 31-34) and leaving through Florida Straits (stations 30-31) are not in agreement. While stations 31-34 are in Yucatan Strait, stations 30-31 are some distance from the Florida Straits and may not completely describe the outflow. The sill depth at Yucatan Strait is about 1600 meters (Sverdrup et al., 1942) and there may be an additional transport below 1000 meters that was not detected in this study because of the reference level selected. Hubertz (1967) and Nowlin and McLellan (1967) have reported an outflow on the Cuban side of the strait in summer and winter respectively. The slope of the isosteres in Yucatan Strait (Figure 12) indicates a southward flow below 500 meters to the east of station 31 during cruise 68-A-8. No complete values are given for this outflow and they will probably not be available until thorough

direct current measurements are made in the deep water of the Yucatan Strait. For this reason, no attempt is made here to balance the inflow and outflow quantitatively.

The interpretation of the classical circulation patterns around areas of high and low dynamic heights can also be used to describe the current patterns in other parts of the Gulf. The dynamic topography in Figure 20 supports the currents indicated by the tongues of low surface salinity discussed in Chapter IV. To the east of the loop current, the area of low dynamic height near station 43 indicates a flow that curves to the left around this station. Part of the south-flowing current to the west of this station curves around it and then proceeds northward toward the Florida Shelf. The flow west from the Mississippi Delta toward the Texas Continental Shelf can not be inferred from Figure 20 because this flow occurred in water too shallow to provide data for this figure. The area of low dynamic height near 26°N and 90°W and the high near 26°N and 93°W are consistent with the southwesterly current in this area indicated by the surface salinity field in Figure 8.

CHAPTER VI

SEA SURFACE TEMPERATURE

A NASA research aircraft was scheduled to fly over the loop current with several types of remote sensors during cruise 68-A-8. This additional information was expected to be used in the analysis of the physical features of the eastern Gulf and particularly the loop current. To utilize this remote sensed data, it was necessary to obtain high quality ground truth data with which to calibrate the remote sensed data. Particular effort was placed in the determination of the horizontal field of temperature. Some remote sensors can only detect the values of the oceanographic elements in the very thin surface layer, or skin, of the ocean. The measurement of sea surface elements by conventional shipboard methods can not determine values of this very thin layer. The size of the instrument and the technique involved result in a value for the top meter of the water column at best.

The two classical methods of determining sea surface temperature are (1) by taking a sample of the sea surface with a bucket and by then measuring its temperature with a thermometer and (2) by reading the water temperature at one of the ship's sea water intakes. Through the years there has been no attempt to standardize the bucket, the thermometer, or the technique, but the bucket temperature is usually regarded as the standard (Roll, 1965). The bucket temperature is a measure of approximately the top meter of water.

Measurements of sea surface temperature on cruise 68-A-8 were made utilizing over 300 hourly bucket temperature readings taken in conjunction with BTs, the surface temperature data from hydrographic stations, and by continuous recording of the sea water intake system.

The continuous temperature and salinity sensing system on the R/V ALAMINOS uses a sea water intake on the centerline of the hull in the forward part of the ship. The intake and sensing equipment are located in the forward hold with the sea water intake about three meters below the sea surface. The system is designed so the forward motion of the ship when making way through the water forces the sea water to flow through the system. When the ship is stopped on a station, a centrifugal pump moves the water.

Figure 22 depicts the agreement between simultaneous readings of sea surface temperature by bucket and intake methods. The 68-A-8 data (curve A) is based on 301 comparisons and shows relatively good agreement with exact agreement occurring 36.2 percent of the time. The maximum errors were -0.7 and +0.6°C and the mean error was -0.05°C. The values (curve B) reported by Roll (1965) were calculated from 5689 measurements and show less agreement.

An infrared thermometer (Barnes IRT-3) was mounted on the bow of the ship in a manner to measure the skin temperature of the water about 5 meters forward of the bow and to one side. Although the shipboard infrared thermometer recorder was calibrated to known temperatures every four hours, it was used to detect surface temperature gradients rather than to derive an actual value for

Figure 22

Frequency of temperature difference in simultaneous readings of bucket and intake temperatures. Curve A from 68-A-8 data, curve B after Roll (1965).

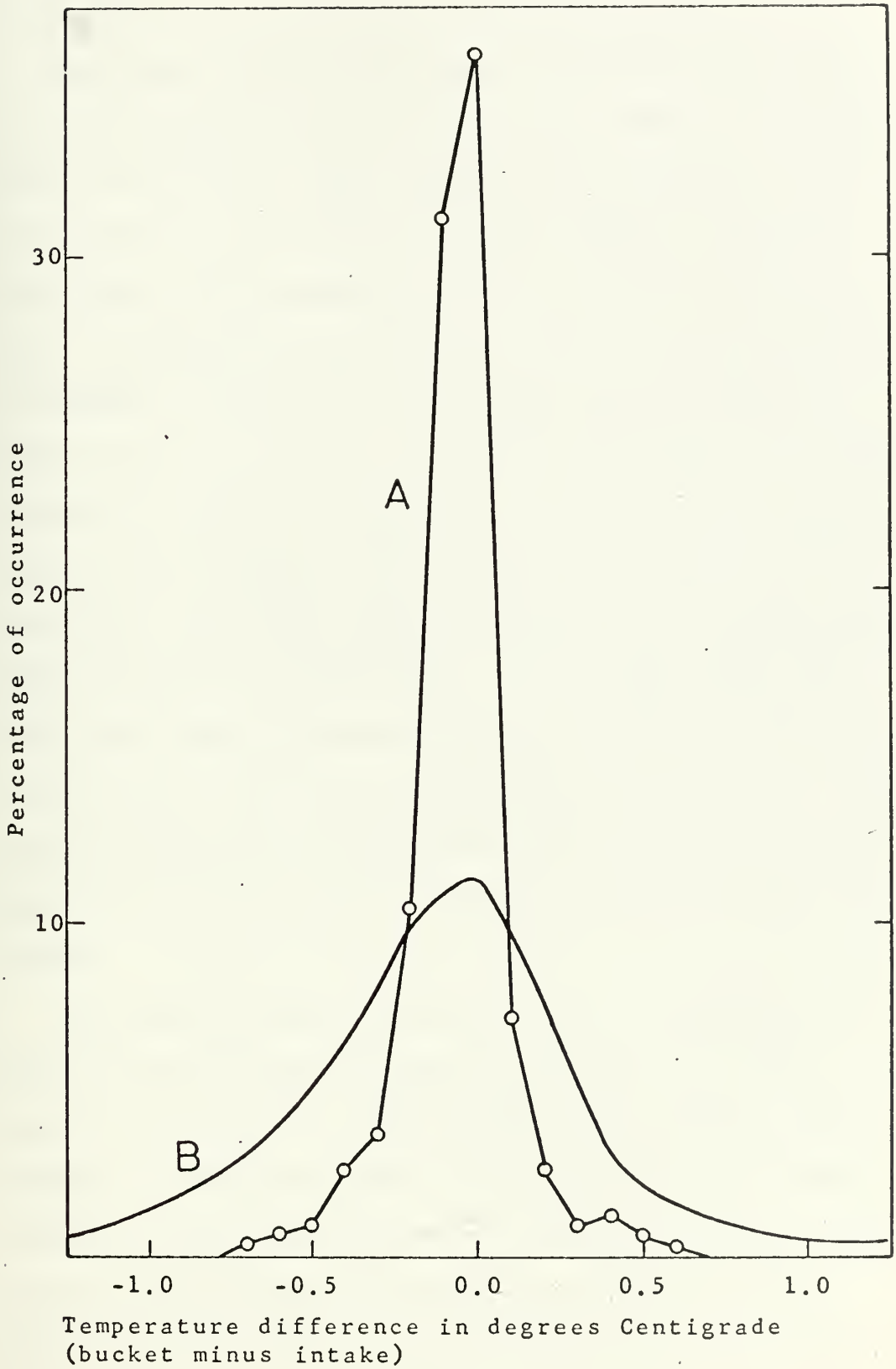
30
20
10
Percentage of occurrence
A
B
-1.0
-0.5
0.0
0.5
1.0
Temperature difference in degrees Centigrade
(bucket minus intake)

temperature.

Sea surface temperature is primarily effected by heat exchange with the atmosphere, convective mixing, solar radiation, mechanical mixing, and advection. Heat exchange with the atmosphere is in turn a function of the sun's declination, latitude, wind force, cloud cover, air/sea temperature difference, humidity, and sea state. Franceschini (1966) studied diurnal variation aboard the R/V ALAMINOS in June, 1965, in the Atlantic Ocean in latitudes similar to those in the Gulf. He found the magnitude of the diurnal variation of sea surface temperature to be 0.7 to 1.6°C. He also reported that the diurnal range of bucket temperatures was 0.2°C greater than that of the intake temperatures. In the afternoon the bucket temperatures would be higher than the intake temperatures indicating a negative gradient at the surface while at night the surface would be cooler and a positive gradient would occur. Table I shows the estimated diurnal variations of sea surface temperature in summer for various latitudinal zones under different weather conditions.

No attempt was made during cruise 68-A-8 to determine the diurnal variation of the sea surface temperature. The values reported by Franceschini (1966) and Wolff et al. (1965) furnish insight as to the expected daily fluctuation in the sea surface temperature field. Faired curves of sea surface temperature versus time are shown in Figures 23 through 27. Each figure covers a three day increment of the cruise while the ship was proceeding

Table I

Estimated magnitudes of diurnal variation of sea surface temperature (°C) in summer (April-September) in various latitudes in offshore areas. After Wolff et al. (1965).

Latitudinal Zones	Wind 0 - 6 knots		Wind 7 - 21 knots		Wind > 21 knots	
	Clear	Cloudy	Clear	Cloudy	Clear	Cloudy
0-20°	1.5	0.8	0.6	0.3	0.2	0.1
20-40°	1.0	0.3	0.4	0.2	0.1	0.0
40-60°	0.5	0.1	0.2	0.1	0.0	0.0
> 60°	0.2	0.0	0.1	0.0	0.0	0.0

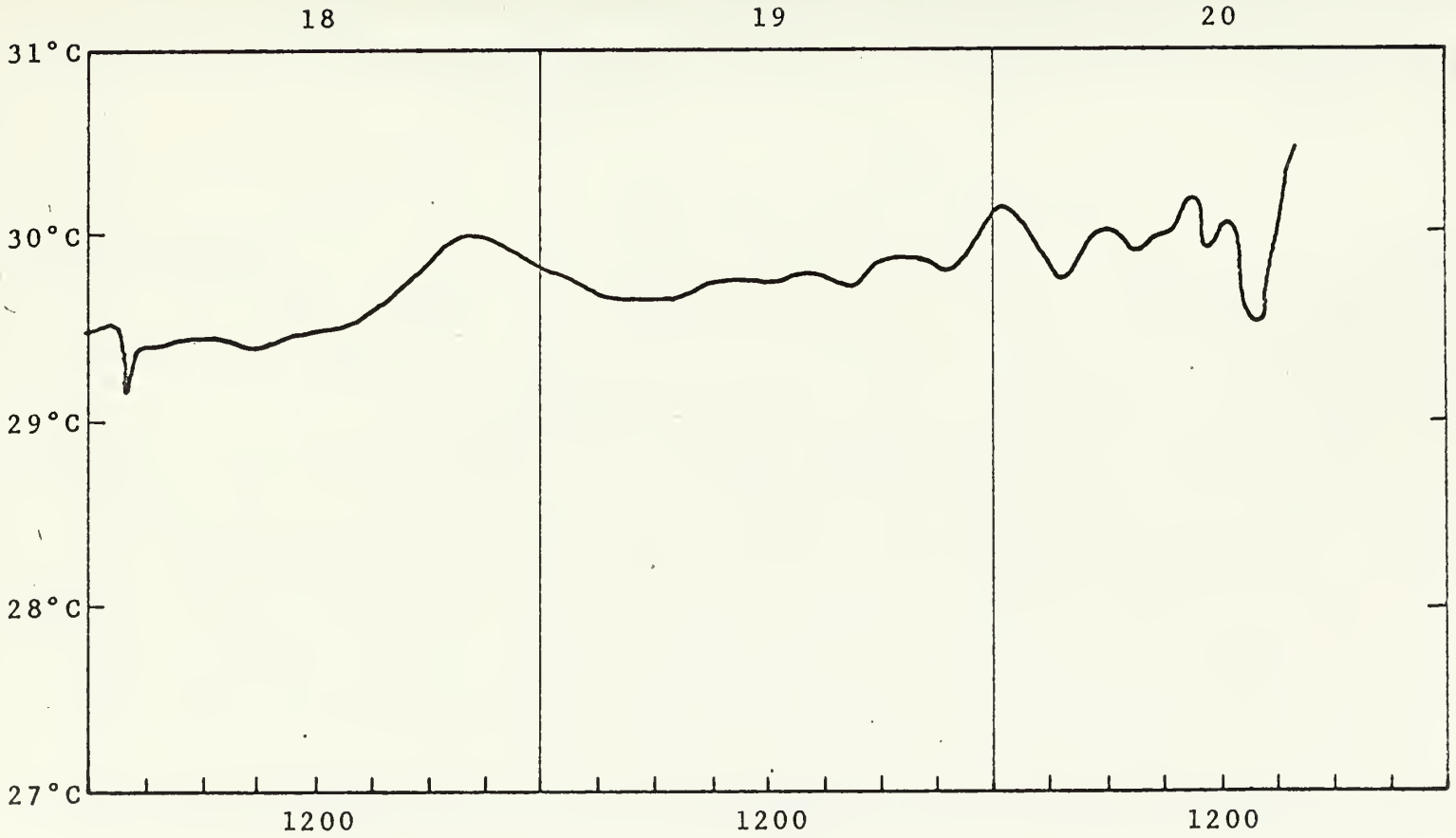

Figure 23
Sea surface temperature, August 18, 1968 through August 20, 1968.
Temperature in degrees Centigrade, time is GMT.

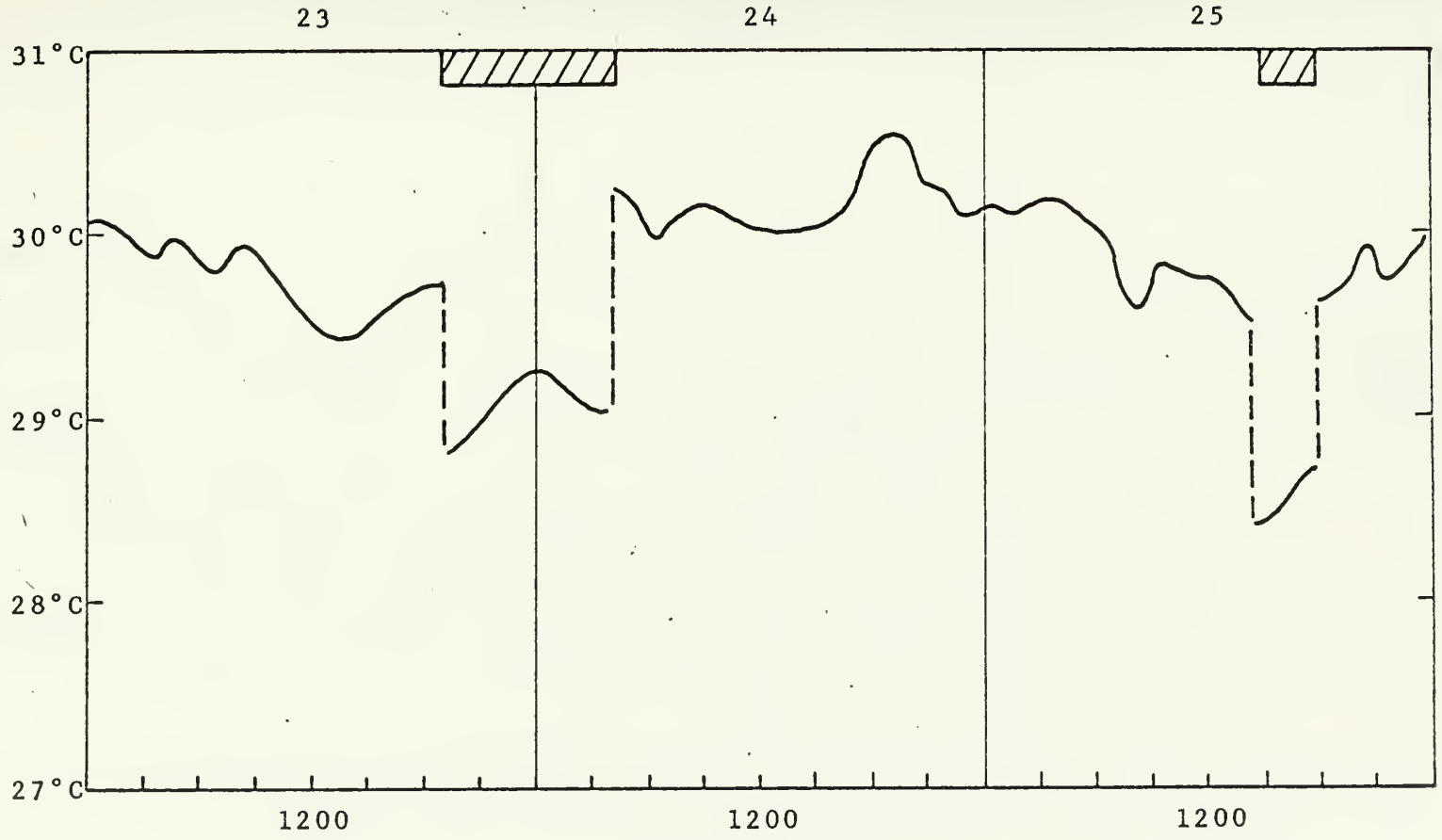

Figure 24
Sea surface temperature, August 23, 1968 through August 25, 1968.
Temperature in degrees Centigrade, time is GMT.

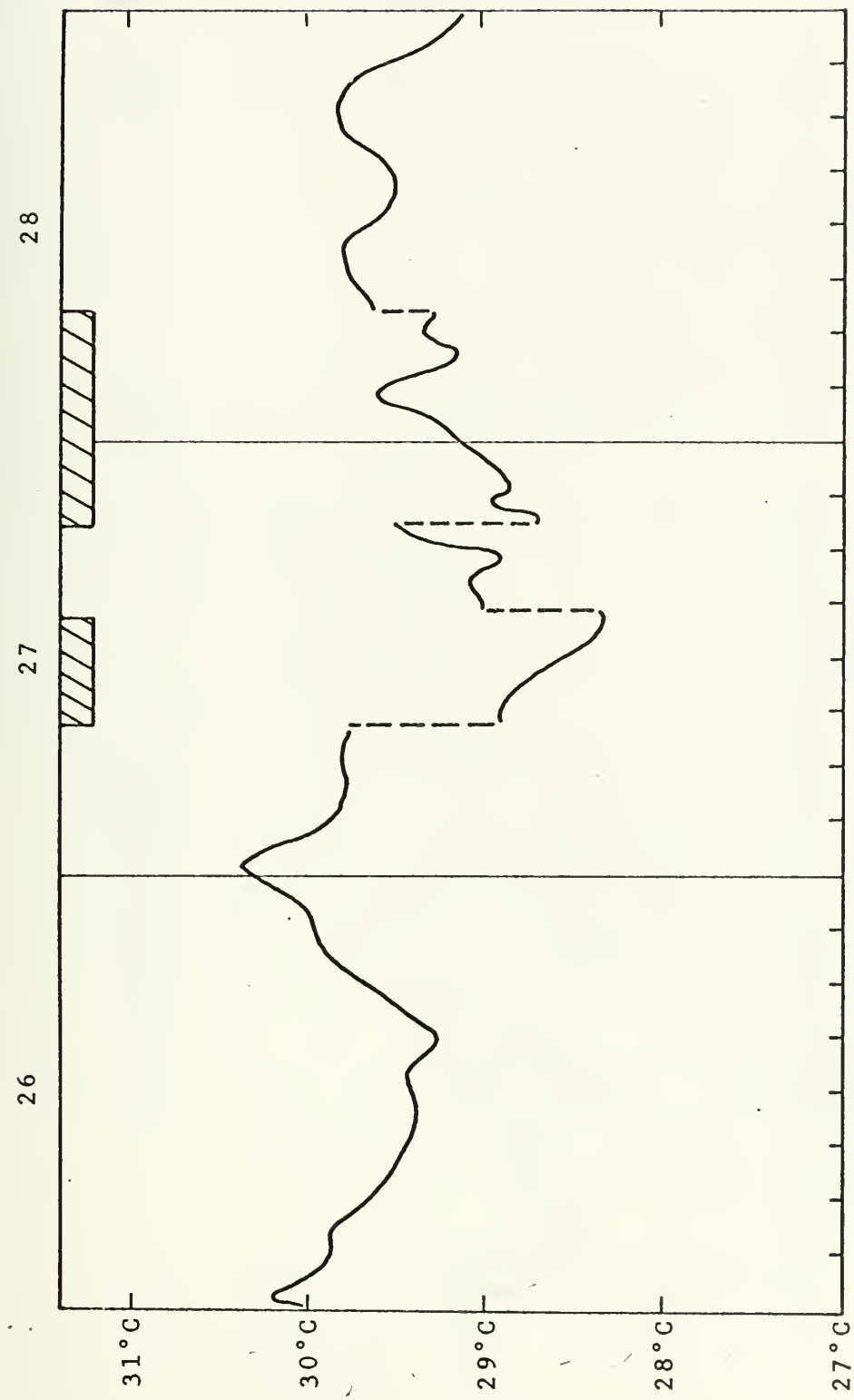

Figure 25
Sea surface temperature, August 26, 1968 through August 28, 1968.
Temperature in degrees Centigrade, time is GMT.

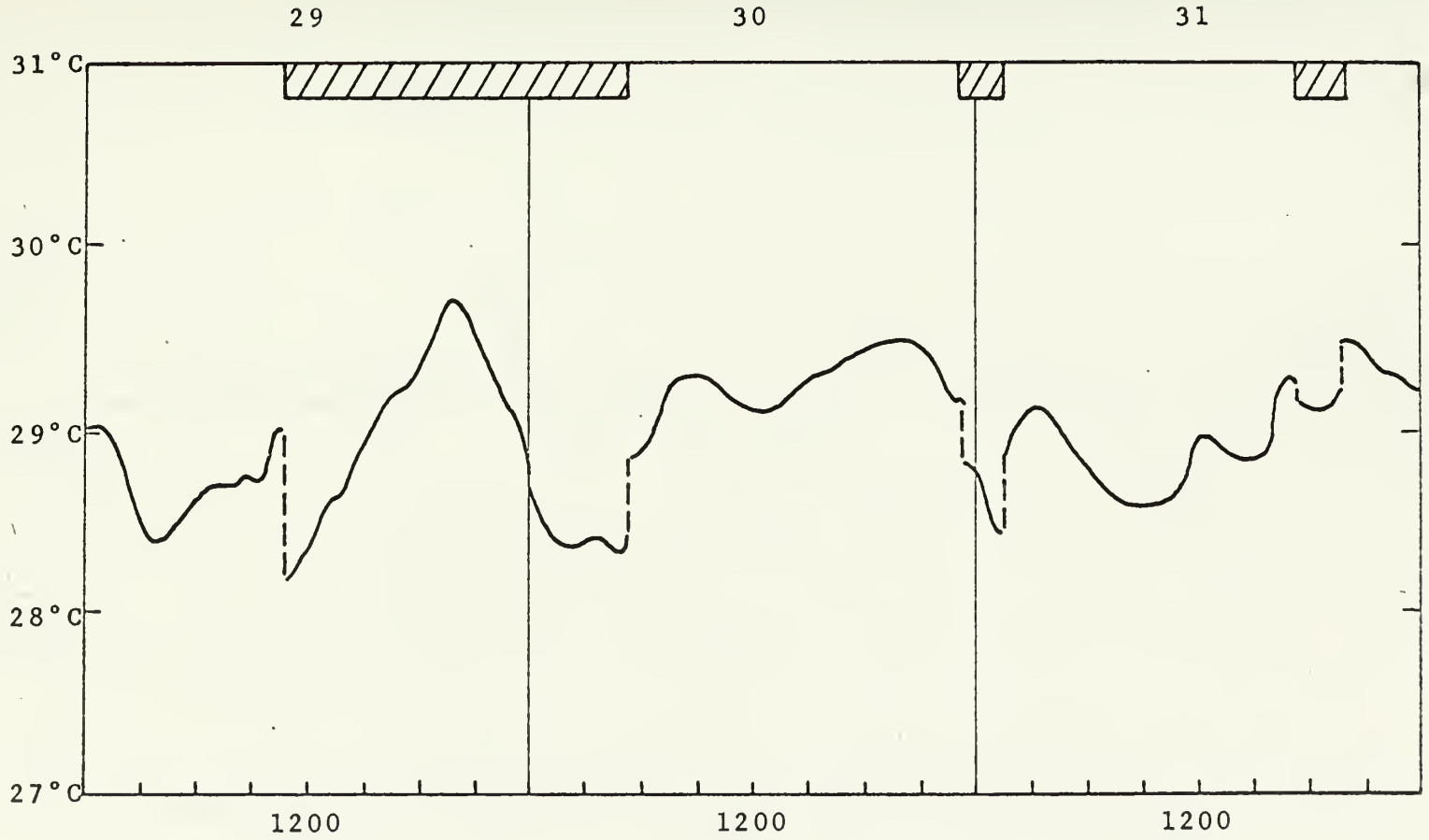

Figure 26
Sea surface temperature, August 29, 1968 through August 31, 1968.
Temperature in degrees Centigrade, time is GMT.

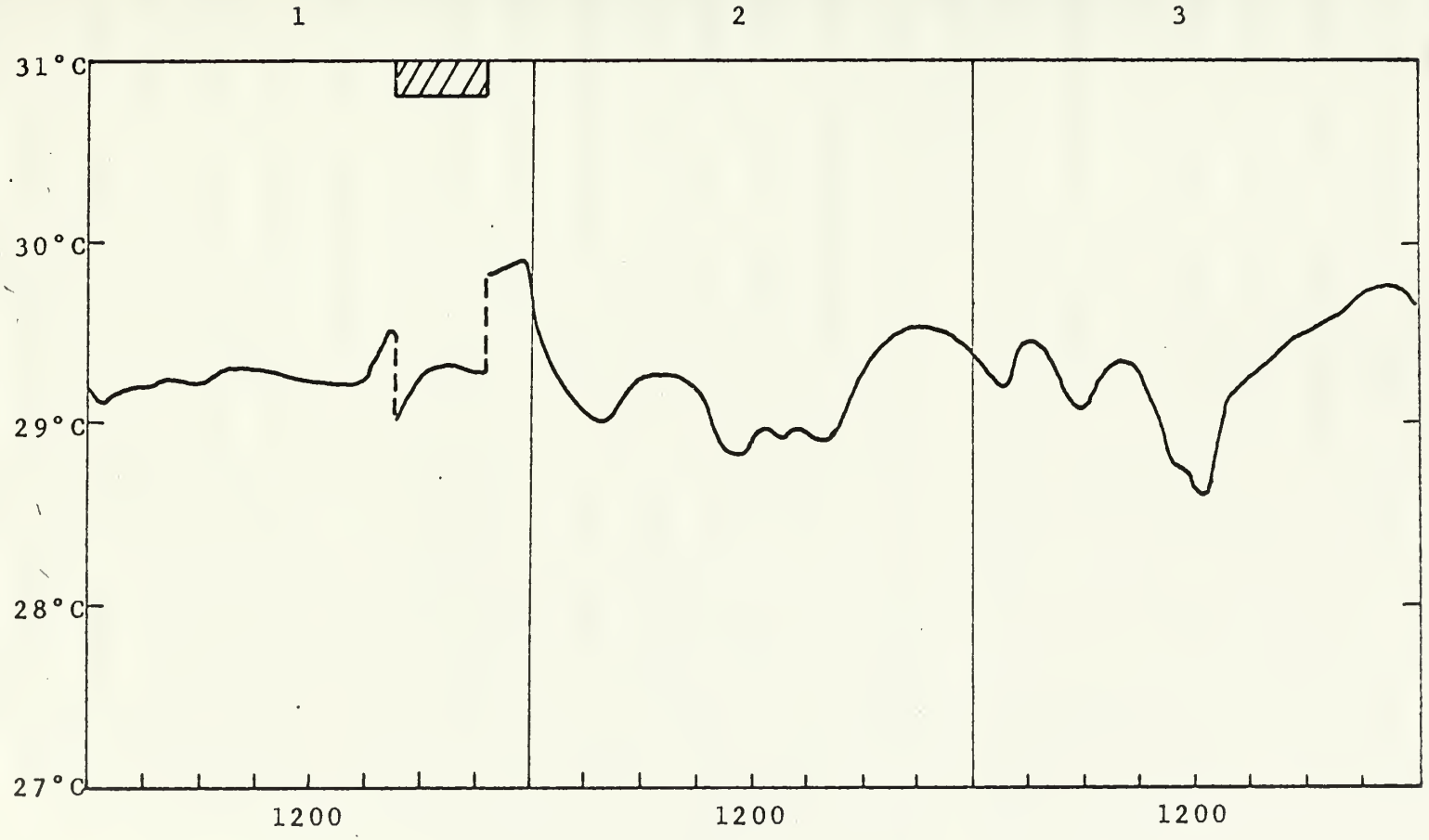

Figure 27
Sea surface temperature, September 1, 1968 through September 3, 1968.
Temperature in degrees Centigrade, time is GMT.

along the cruise track (Figure 1). Temperature data were obtained from bucket temperature, surface temperature from hydrographic stations, and from hourly averages of intake temperature. In the process of fairing these data into a single smooth curve, the hourly averages of intake temperature were given the most weight. This was done because that system is independent of personnel errors and individual measuring techniques, because it provided a continuous record, and because it was in good agreement with the simultaneous bucket temperatures.

The temperature data obtained can not be thought of as showing the diurnal variation because the ship did not remain in the same position. However, Figures 23 through 27 do show a variation that is somewhat similar in nature to the expected diurnal variation. The data in Figure 23 terminated at 1600 GMT August 20 as the ship entered the Mississippi River. It resumed again at 0000 GMT on August 23 when the ship left the river. Generally, the highest sea surface temperature was found between 2000 and 0000 GMT (1500 to 1900 local time) and the lowest temperature occurred in the early morning (local time) around sunrise.

The most significant feature, however, is the sudden downward displacement (to lower temperatures) of the curve at times. This displacement is indicated by a vertical dashed line and is seen in Figures 24 through 27. These displacements range from 0.3 to 1.1°C and were observed on all the temperature sensors including the shipboard infrared thermometer. The general shape of the sea

surface temperature curve is preserved in the displaced portion of the curve.

The areas of lower surface temperature were found only in the eastern Gulf in the region of flow of the loop current. Figure 28 shows an areal picture of the location of this feature with the shaded area indicating the cooler surface water. Due to its shape and location, this feature seems to be associated with the loop current. Wolff et al. (1965) have stated that sharp changes in sea surface temperatures may be caused by upwelling along a coast or a divergence line and may be found at current boundaries. Table II lists the temperature change measured by the two continuously recording temperature sensors as well as the time and location of the change.

The region of the colder surface water is found above the loop current with two exceptions. At Campeche Bank and just north of it, the colder water is about 40 nautical miles (74 kilometers) west of the loop current. At the northeastern corner of the loop, the colder water is about 40 nautical miles east of the current. This displacement is attributed to the deep waters of the current 'feeling' the bottom in these areas and being somewhat restricted by it while the surface water is free to flow over the shelf.

The temperature changes and the gradients are greatest along the northern portion of the loop and are weakest in the portion just south of the northeastern corner. The portion of the colder surface water bounded by double lines in Figure 24 is the area

Figure 28

Horizontal distribution of colder surface water, cruise 68-A-8.

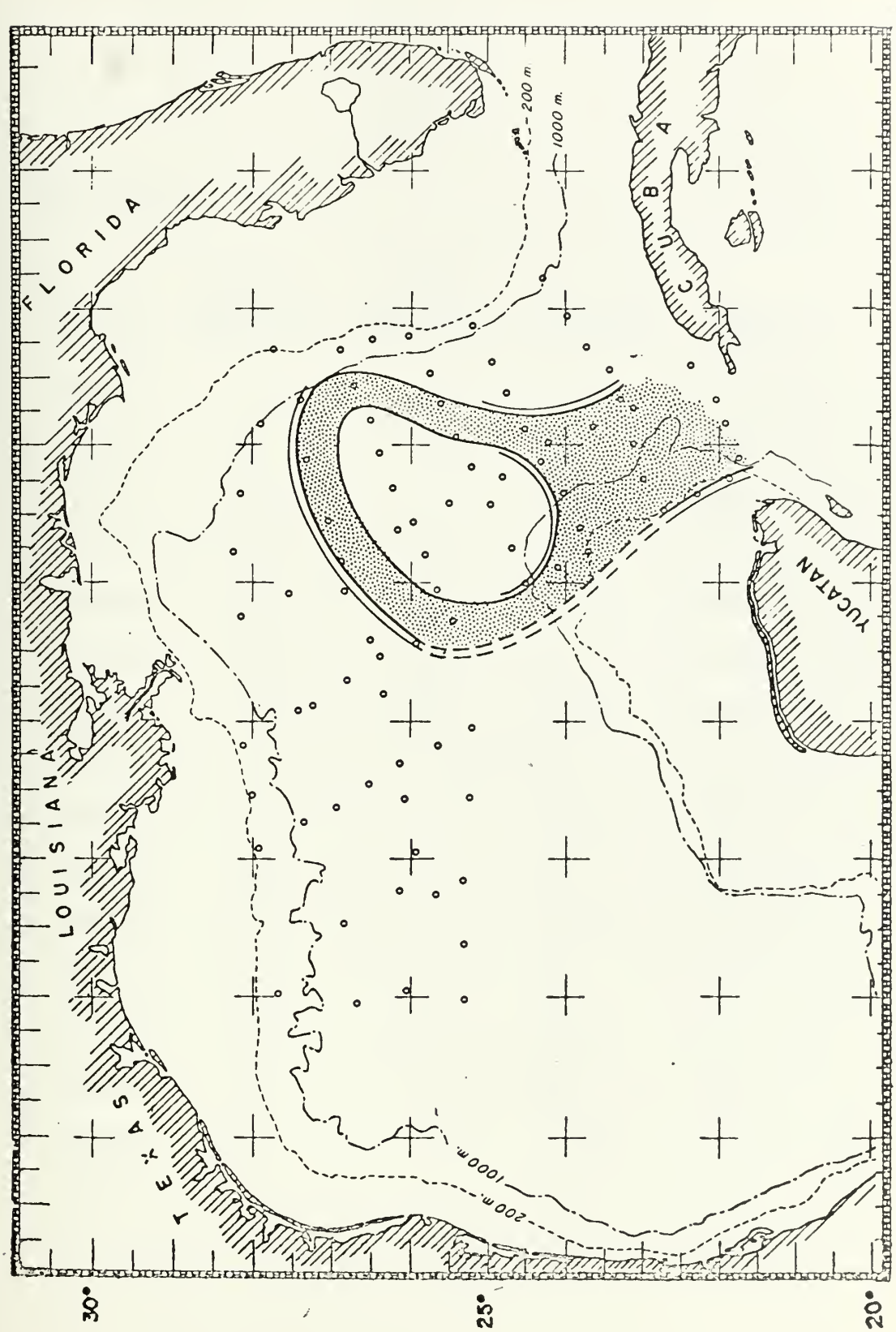
FLORIDA
LOUISIANA
TEXAS
CUBA
YUCATAN
200 m.
1000 m.
1000 m.
200 m.
80°
85°
90°
95°
30°
25°
20°

Table II

Detection of the colder water at the surface of the loop current, cruise 68-A-8.

Date/time (GMT)	Intake Temperature Change (°C)	IRT Temperature Change (°C)	Direction of Change	Remarks
23/1905	0.9	1.0	Down	Near BT 71
24/0430	0.7	0.7	Up	After BT 78
25/1455	0.8	1.1	Down	Before Sta 24
25/1750	0.5	0.4	Up	Before BT 107
27/0840	0.6	0.4	Down	Before BT 135
27/1430	0.6	0.6	Up	Before BT 140
27/1924	1.0	0.9	Down	After BT 143
28/0715	0.6	*	Up	After BT 151
29/1100	0.7	0.7	Down	Before BT 173
30/0515	0.8	*	Up	After BT 187
30/2215	0.3	*	Down	After Sta 58
31/0115	0.5	*	Up	Before Sta 59
31/1715	0.3	*	Down	After BT 216
31/1945	0.5	*	Up	Before BT 218
01/1630	0.5	*	Down	Before BT 235
01/2136	0.7	*	Up	Before BT 239

* No temperature change detected.

where the temperature change is greater than 0.5°C. The possibility of using this feature to detect the presence of the loop current will be discussed in Chapter VIII.

CHAPTER VII

SOUND VELOCITY

Background

Cruise 68-A-8 provided data to determine sound velocity* profiles for a number of stations in close proximity in the eastern Gulf of Mexico. The variation in these sound velocity data due to the variation in geographic position within the right- or left-hand water of these stations is negligible but that due to the occurrence of right- or left-hand water is not. This cruise provided data with which to investigate sound velocity profiles based on these two classifications. In the past, most sound velocity profiles in the Gulf have been evaluated or grouped on the basis of geographic position alone. Considering the variation in the loop current, it can be seen that the water at a fixed location may change significantly as the loop intrudes into the Gulf, spreads out, and then decays. The location may first be to the left of the current (in left-hand water), then in the current, and finally to the right of it (in right-hand water). For this reason, the sound velocity profiles and sound propagation characteristics in the right- and left-hand water will be investigated ard compared. Wilson's equation (McLellan, 1965: equation 16.3) was used to determine sound velocity

---

* Popular usage favors the term 'velocity' for 'speed' of sound even though it is a scalar quantity. For this reason, the term 'velocity' will be used here in place of 'speed'.

in this study.

At the present time, sound is the most efficient method for transmitting intelligence through the ocean. It is used for underwater communications, locating fish, depth finding, subsurface profiling, navigation, and for antisubmarine warfare. One of the most important factors influencing the transmission of sound waves through large bodies of water is the effect due to refraction caused by variations in the sound velocity. Refraction both interferes with the use of acoustic systems and permits efficient long range propagation under different conditions. The propagation of sound is also effected by internal waves, turbulence, and biologics.

The velocity of sound is dependent on three major factors: temperature, salinity, and pressure (depth). Near the surface and in the thermocline, temperature is the dominant factor in the sound velocity profile (SVP). An increase in temperature of 1.0°C at 28°C results in a velocity increase of 2.2 m/sec. The same change at 4°C causes a velocity change of 4.1 m/sec.

Sound velocity increases with increasing salinity at a rate of approximately 1.4 m/sec for each 1.0^{o}/oo change in salinity at 35.0^{o}/oo. The variations due to salinity are relatively minor except at the sea surface where evaporation, rainfall, and runoff may create large gradients. The range of surface salinity in the offshore areas of the Gulf of Mexico in August, 1968, was less than 0.6^{o}/oo. Larger variations were found near the Mississippi

Delta. (See Figure 8.)

Sound velocity increases with depth at a fairly uniform rate of 0.018 m/sec per meter of depth. In the deep water where the temperature and salinity gradients are small (below 1000 meters), pressure becomes the dominant factor in the sound velocity profile.

Sound waves produced by depth finders are directed vertically downward and are, therefore, not refracted. However, since depth finders assume a constant sound velocity (usually 1463 or 1500 m/sec), errors result when the mean vertical sound velocity is different from the constant employed. An erroneous depth results when the travel time of the echo is converted to distance. Mathews' Tables provide corrections which when applied to 'fathometer depth' give the true depth. Mathews divided the world ocean into 52 areas of similar temperature and salinity stratification. The Gulf of Mexico has been divided into three areas. Mathews' area 16 includes the water surrounding the Mississippi Delta, area 18 includes the water in Yucatan Strait and just north of it, and area 17 represents the rest of the Gulf. The depth corrections listed for areas 17 and 18 were similar to the corrections required for the left- and right-hand water respectively. However, the boundaries of these areas will change significantly during the year as loop current grows and decays. Mathews' Tables are not applicable for shelf regions where strong local differences and seasonal variations of the mean vertical sound velocity may occur (Dietrich, 1963). The more common practice today is to determine depth corrections from

hydrographic station data obtained in that area. Ryan and Grim (1968) have reported the formulation of a computer program to do this.

The propagation of sound in directions other than the vertical is more complicated. The shadow zone and the sound channel are two features that may occur and these will have a significant effect on propagation. Sound waves constricted to a sound channel do not diverge with spherical spreading as in the case of an iso-velocity profile but diverge cylindrically. Low frequency sound, which suffers little absorption, can be propagated great distances under these conditions. This is a very important consideration in underwater communications and antisubmarine warfare.

Sound channels are commonly found in two areas of the water column. They may occur at or near the surface and at depths of about 1000 meters. A layer of well mixed water is usually found at the surface. Under these conditions, the only change in sound velocity with depth is due to the change in pressure which causes sound velocity to increase with depth. The result is a positive velocity gradient and, therefore, a surface sound channel. Surface cooling at night or an outbreak of cold air are other factors which lead to the formation of surface sound channels.

The deep sound channel is a permanent feature in almost all deep oceanic water. The water temperature decreases with increasing depth until it reaches its maximum density at about 4°C. This occurs near 1000 meters in the Gulf of Mexico. Above this depth,

the temperature component of sound velocity is the dominant factor and this results in a negative velocity gradient. Below this depth, temperature gradients are small and pressure is the dominant component of sound velocity resulting in a positive velocity gradient to the ocean bottom. The resultant velocity minimum is the axis of the deep sound channel.

Sound Velocity Profiles

The hydrographic stations for cruise 68-A-8 have been classified as right-hand or left-hand water in Figure 3. It has been shown in Chapter III that the physical properties in the left-hand water are found at a depth shallower than that of the same properties in right-hand water. The effects of these temperature and salinity differences combine causing SVPs that are significantly different in the right- and left-hand water. In the upper 1200 meters the sound velocity in the left-hand water at a given depth is always considerably less than that in right-hand water. This can be seen by comparing the SVPs in Figures 29 and 30 which show the SVP for right- and left-hand water respectively. In addition to the overall shape of the profile, there is a much wider range of velocity near the top of the thermocline in the left-hand water. The difference between the extreme profiles in the right-hand water is much less in this area.

To describe the seasonal variation in SVP, a number of stations in right- and left-hand water were selected from winter cruises

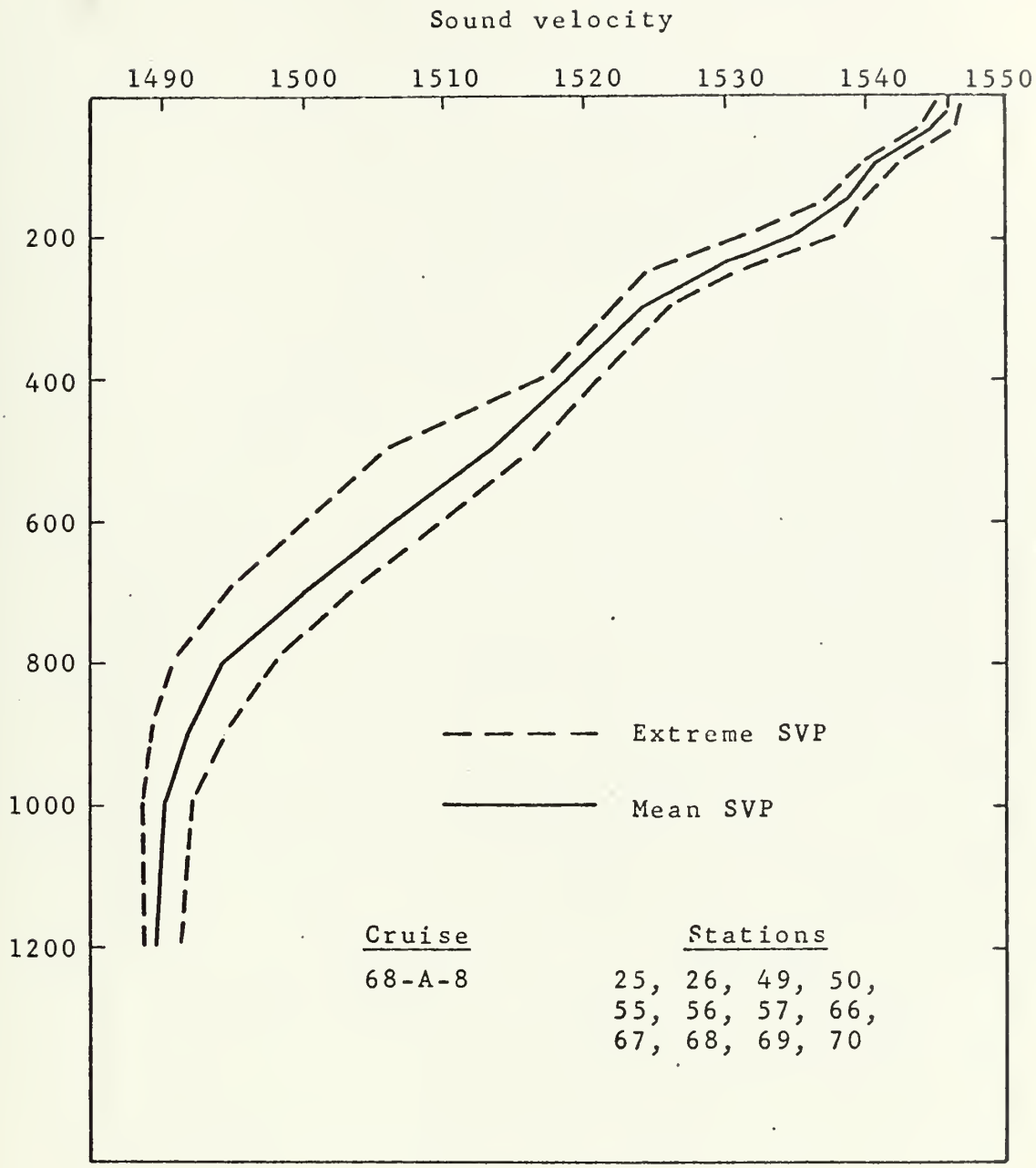

Figure 29

Mean and extreme values of sound velocity profile for 12 stations in right-hand water in the eastern Gulf of Mexico in summer, cruise 68-A-8. Depth in meters, sound velocity in meters per second.

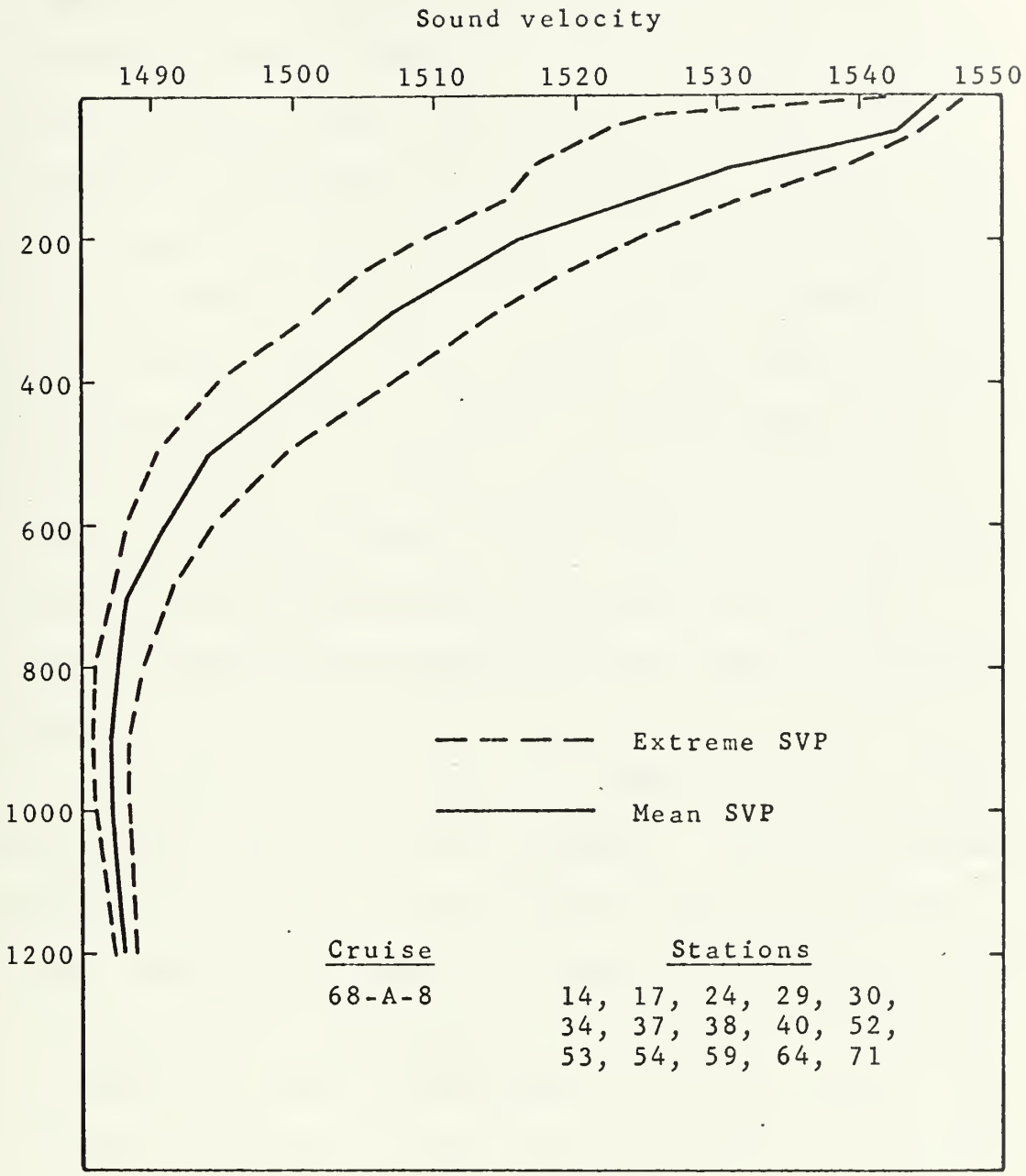

Figure 30

Mean and extreme values of sound velocity profile for 15 stations in left-hand water in the eastern Gulf of Mexico in summer, cruise 68-A-8. Depth in meters, sound velocity in meters per second.

cruises in the Gulf of Mexico. The hydrographic station data were obtained from Leipper (1968c and d) and were classified in the same manner as the 68-A-8 data. The cruise and the stations used are identified in each figure used in the comparison. Admittedly, very few stations in both winter and summer were used for SVP comparisons. During the winter, there were very few stations in right-hand water due to the early stage of loop development. The desire to use only data that were gathered and reduced in the same manner further restricted the number of stations available. Even though few stations were used, the SVPs were very consistent with respect to season and station classification. This data will provide an initial comparison of the seasonal variation of SVPs in the Gulf of Mexico.

Six stations representative of the right-hand water in winter were selected from cruises 66-A-3 and 68-A-2. The SVPs are shown in Figure 31. The summer and winter profiles (Figures 29 and 31) reveal large differences above 150 meters due to the seasonal change in temperature in the mixed layer. From 150 meters to 1200 meters the range of the summer SVPs included all the winter profiles. The mean SVP in the winter averaged 2 m/sec lower from 150 to 450 meters and 4 m/sec lower from 450 to 800 meters. There was little or no difference in the mean velocities below 800 meters. The axis of the deep sound channel is generally deeper than 1200 meters.

Five stations were selected from cruise 68-A-2 to represent the left-hand water in winter, and the profiles are shown in

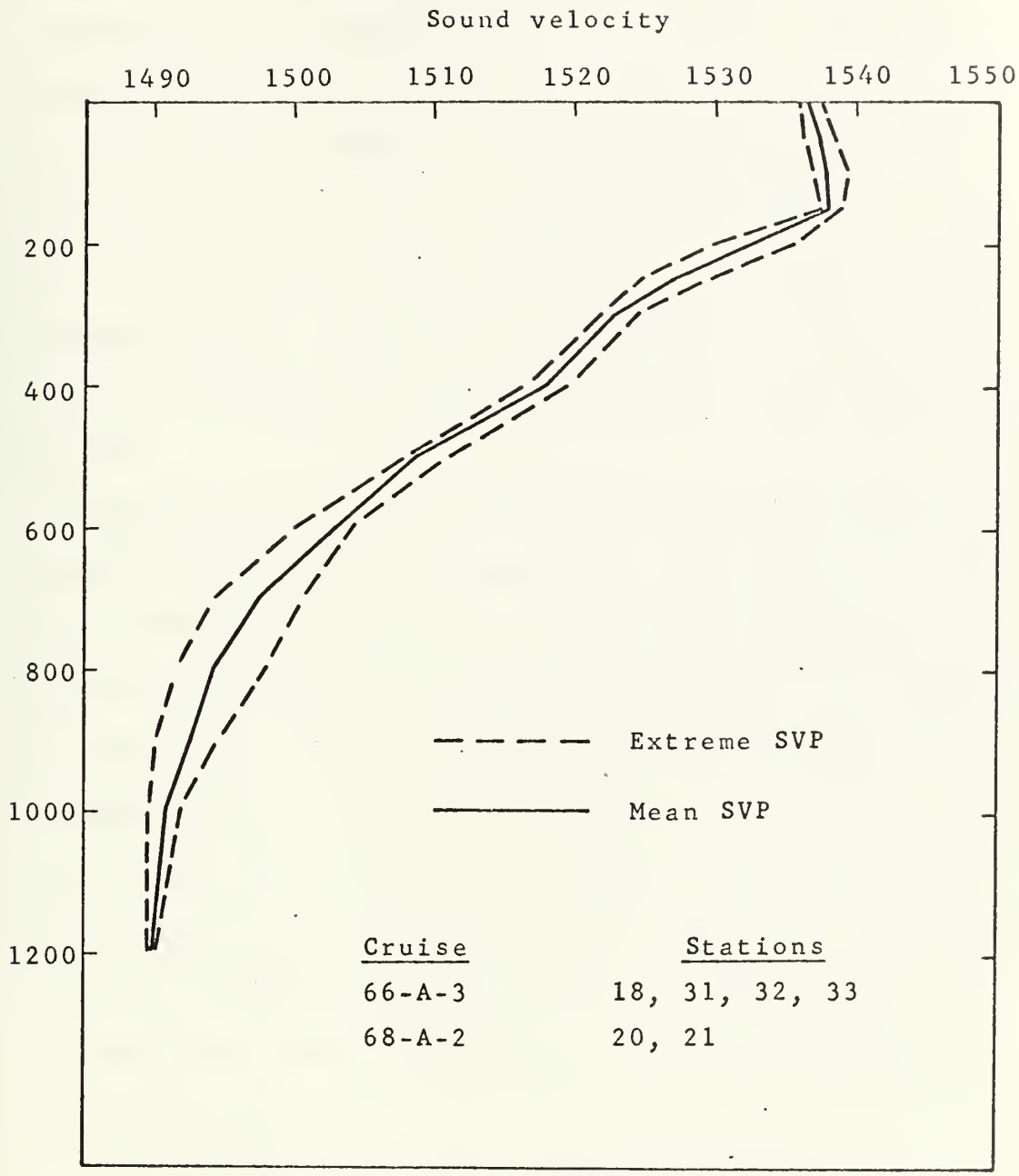

Figure 31

Mean and extreme values of sound velocity profile for 6 selected stations in right-hand water in the eastern Gulf of Mexico in winter, cruises 66-A-3 and 68-A-2. Depth in meters, sound velocity in meters per second.

Figure 32. In this case, the values of sound velocity always lie to the left (lower velocity) of the summer profiles. The greatest difference in the shape of the profile occurs above 150 meters. At 150 meters the mean difference in velocities is 10 m/sec. This difference decreases rather uniformly to zero at 1200 meters. The SVP in left-hand water appears to be effected by seasonal change to a deeper depth than that in the right-hand water. The axis of the deep sound channel in left-hand water is found at about 900 meters all year.

The depth of the surface sound channel, which is influenced strongly by the depth of the mixed layer, varies markedly. In the right-hand water, the depth of the surface sound channel was found to vary from an average of 140 meters in the winter to 41 meters in the summer. This is due to lower air temperatures, higher winds, and deeper mixing in the winter. In contrast, the average depth of the surface sound channel in the left-hand water varies only from 18 meters in the summer to 24 meters in the winter. Mechanical mixing in the left-hand water is restricted to these depths because the top of the seasonal thermocline is closer to the surface in the left-hand water.

Diurnal changes in the SVP are caused by temperature changes in the surface layers due to solar heating, mixing, and evaporation. When this daily fluctuation produces negative temperature gradients at the surface due to insolation, it is called 'afternoon effect'. This results in the downward refraction of sound rays and a

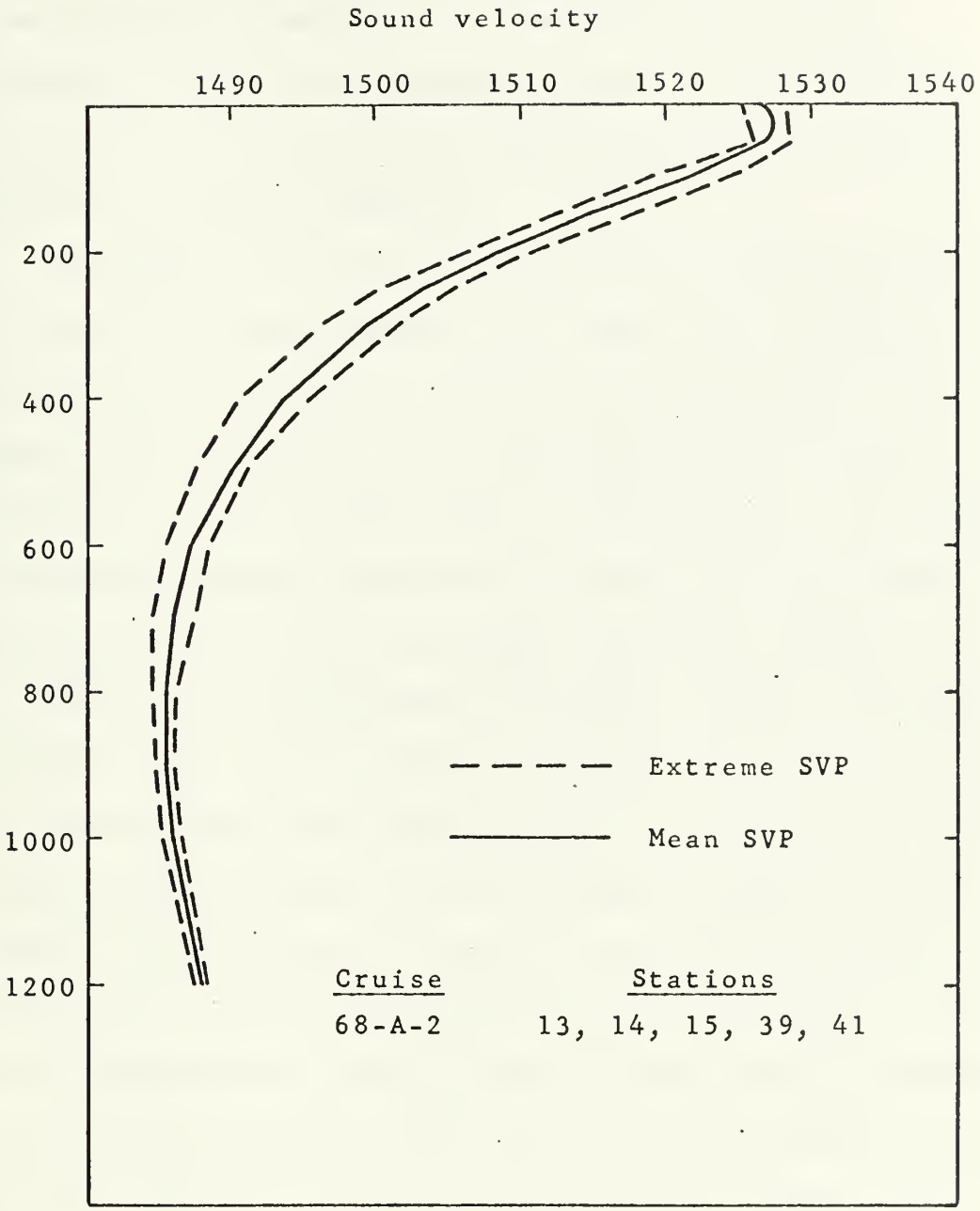

Figure 32

Mean and extreme values of sound velocity profile for 5 selected stations in left-hand water in the eastern Gulf of Mexico in winter, cruise 68-A-2. Depth in meters, sound velocity in meters per second.

reduction in near surface sound ranges. Shadow zones occur under these circumstances and result in areas where little sound is propagated. This is more prevalent in summer (in north latitudes) than winter due to warmer surface temperatures and larger diurnal variations of surface temperature.

Two segments of the 68-A-8 cruise track were chosen to show the nature of the daily change in SVP (Figure 33). This figure does not represent the diurnal variation of SVP but rather the change in SVP that occurs over a 24 hour period while a ship is proceeding in water of similar physical characteristics. The figure is considered typical of sound velocity conditions in the right- and left-hand water in the late summer in the Gulf of Mexico.

Based on the classification of stations in Figure 3, stations 3 through 7 were selected to represent left-hand water while stations 57, and 66 through 70 were chosen to typify right-hand water. An attempt was made to select stations occupied in sequence and that covered a 24 hour interval. Station 2 could not be used because both reversing thermometers at the 20 meter depth failed, so there was no temperature and, hence, no value of sound velocity available at that important depth. Station 57 was not in time sequence with the other right-hand stations but was included to provide a SVP for the early afternoon (local time). The distribution of right-hand water was such that no segment of the cruise track covered a 24 hour period within this water.

The daily changes in the near surface SVP are shown in

Figure 33

Variation in sound velocity profile in right-hand water (top) and left-hand water (bottom) in the Gulf of Mexico in summer, cruise 68-A-8.

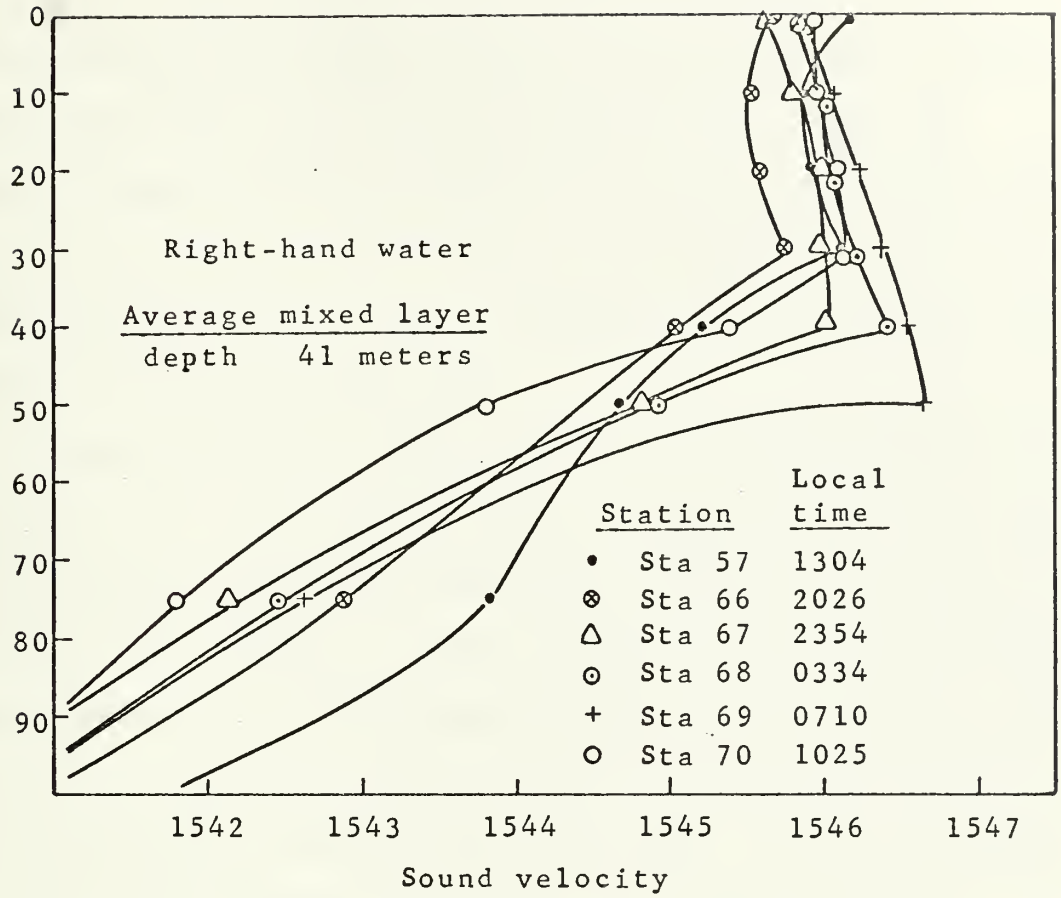
0
10
20
30
40
50
60
70
80
90
Right-hand water
Average mixed layer
depth 41 meters
Station
Local time
• Sta 57 1304
⊗ Sta 66 2026
△ Sta 67 2354
⊙ Sta 68 0334
+ Sta 69 0710
○ Sta 70 1025
1542
1543
1544
1545
1546
1547
Sound velocity

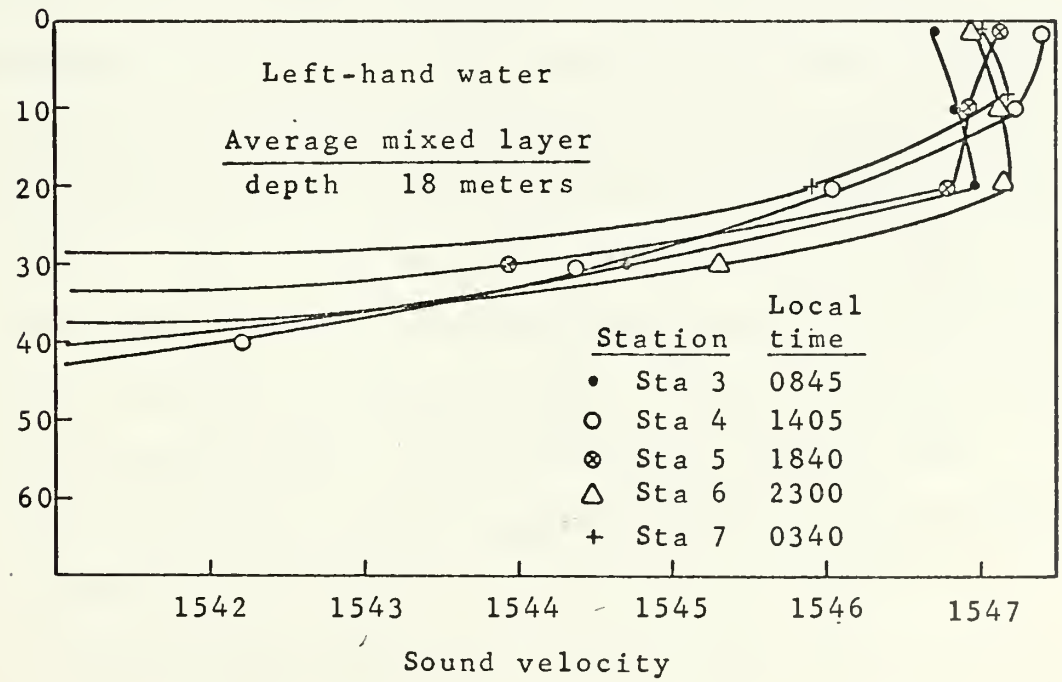
0
10
20
30
40
50
60
Left-hand water
Average mixed layer
depth 18 meters
Station
Local time
• Sta 3 0845
○ Sta 4 1405
⊗ Sta 5 1840
△ Sta 6 2300
+ Sta 7 0340
1542
1543
1544
1545
1546
1547
Sound velocity

Figure 33. This variation can be seen more clearly in the left-hand water and only that part of the figure will be discussed. Figure 34 shows the change in sea surface temperature (from Figure 23), surface sound velocity, and depth of the surface sound channel for the same stations in left-hand water as in Figure 33. The figures and discussion will use local time which is five hours earlier than GMT due to daylight saving time.

Just after sunrise (station 3) the sea surface temperature is rising but it is still cooler than at depths below it. This results in a positive sound velocity gradient in the upper 20 meters and hence a sound channel. By early afternoon (station 4) sea surface temperature and sound velocity have reached a peak. The result is a negative sound velocity gradient from the surface to the axis of the deep sound channel at about 900 meters. This is an example of the afternoon effect; the surface sound channel has been destroyed. In the early evening (station 5) the surface temperature is decreasing but the velocity gradient is still negative. Mixing has changed the shape of the SVP and reduced the negative velocity gradient. In the early part of the night (station 6) the sea surface temperature is approaching its minimum value and the sound velocity gradient has become positive. A surface sound channel has been established again. In the early morning (station 7) sea surface temperature is still relatively cool and the sound channel is present.

The sea surface temperature follows a similar pattern in the

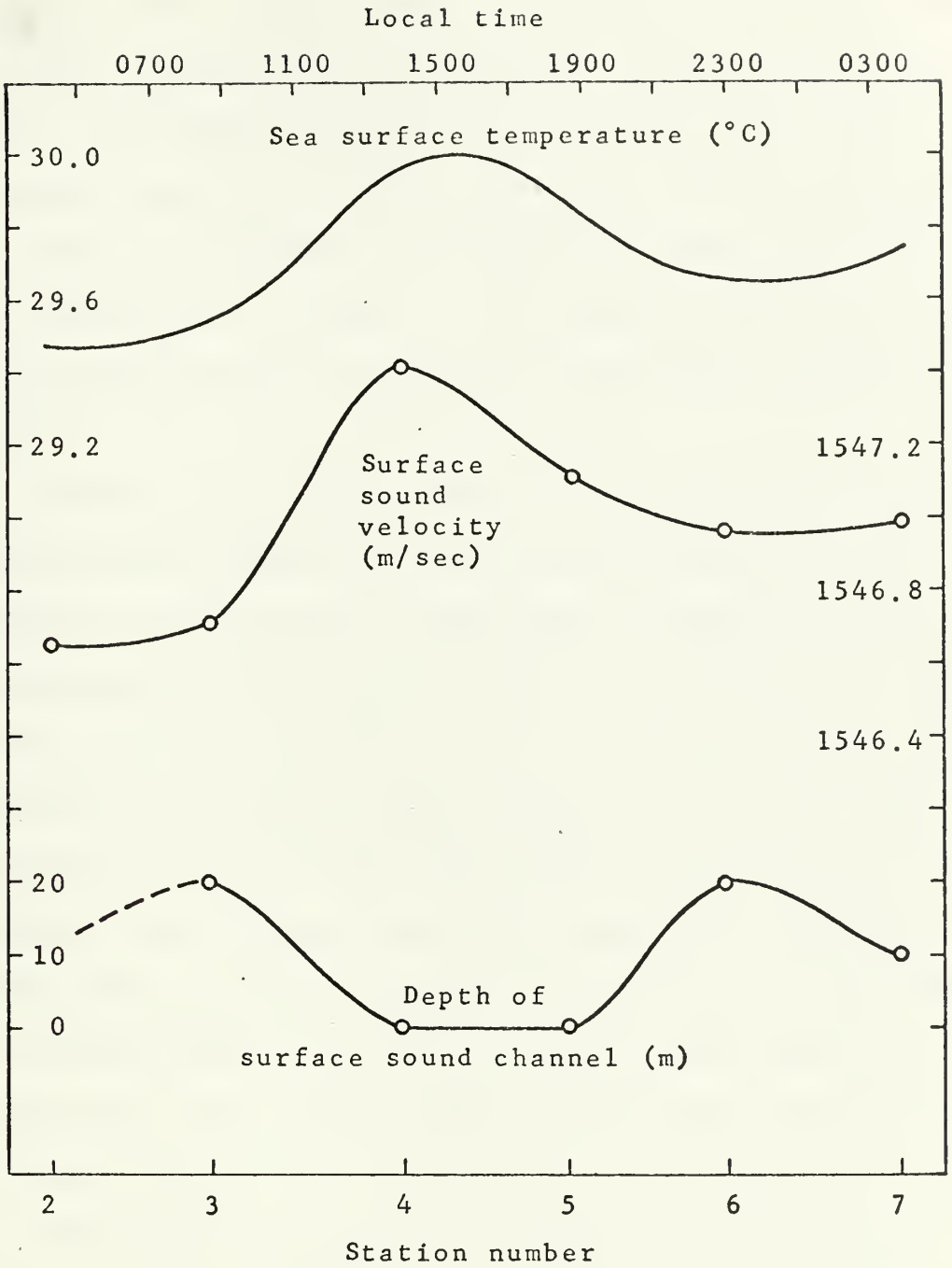

Figure 34

Variations of sea surface temperature, surface sound velocity, and depth of the surface sound channel in left-hand water in the Gulf of Mexico in summer, cruise 68-A-8.

right-hand water. In this water with its deeper mixed layer, there was never a negative temperature gradient through the entire mixed layer. The bottom of the mixed layer was always warmer than at some depth above it in the water column. The result was that there was always a sound channel in the right-hand water and the afternoon effect did not eliminate it. At times, the axis of the sound channel was found about 10 meters below the surface (stations 57 and 66).

The time of the maximum surface sound velocity and of the maximum surface temperature occurred between 1800 and 2030 GMT (1300 and 1530 local time) in August, 1968. ALAMINOS was at sea during this time of day on fifteen days during cruise 68-A-8. The ship was in 'coastal' water on five days, in right-hand water three days, and in the left-hand water on seven days. Table III shows the occurrence of the surface sound channel during the time of the afternoon effect. When the ship was in right-hand water a surface sound channel was present throughout the period in each case. When the ship was in left-hand water, the surface sound channel disappeared due to the afternoon effect on five of the seven days. On the other two days, the vertical distribution of temperature from BTs taken between stations shows a negative temperature gradient indicating that the sound channel probably disappeared between the times for which station data are available. The BTs were studied to see if the same thing happened in the right-hand water, but there was no indication of it. No attempt was made to determine a

Table III

Presence of surface sound channels in the afternoon, cruise 68-A-8.

Date	Water Classification	Sound Channel Disappears	Station	Local Time
18 Aug	LH	Yes	4	1405
19	C	No	9	1315
20-22	In port, New Orleans, La.			
23	LH	Yes *	-	-
24	C	Yes	20	1515
25	RH	No	25	1530
26	LH	Yes	30	1422
27	LH	Yes	37	1522
28	C	No	44	1440
29	RH	No	50	1427
30	RH	No	57	1304
31 Aug	LH	Yes	64	1401
1 Sep	LH	Yes	71	1435
2	C	No	78	1510
3	C	No	84	1344
4 Sep	LH	Yes #	-	-

C - coastal water, LH - left-hand water, RH - right-hand water. See Chapter III for station classification and description.

* BT 72, taken at 1500 local time, shows a negative thermal gradient extending from the surface into the thermocline.

BT 295, taken at 1400 local time, shows a negative thermal gradient extending from the surface into the thermocline.

pattern in the coastal water due to the large variations in temperature and salinity.

From this limited amount of data, it appears that one may expect the surface sound channel to disappear in the left-hand water in the summer due to the afternoon effect but that it will always be present in the right-hand water. This is attributed to the fact that the mixed layer depth in the right-hand water averages 41 meters, whereas in the left-hand water it is only 18 meters. The afternoon heating of the water will create a continuous negative thermal gradient and negative velocity gradient in the left-hand water, but it will effect only the upper half of the mixed layer in right-hand water. The time of the afternoon effect usually occurred between 1300 and 1530 local time.

CHAPTER VIII

REMOTE SENSED DATA

Background

The main objective of remote sensing in the field of ocean science is to gather synoptic data over large areas of the ocean. The investigation of the remote sensors and remote sensing techniques in ocean science is a task of the Space Oceanography Project (SPOC) which is part of the National Aeronautics and Space Administration's Earth Resources Survey Program. The oceanographic portion of this program is administered for NASA by the U. S. Naval Oceanographic Office.

The potential of aircraft surveys in the fields of marine meteorology and oceanography has been recognized for some time. Aircraft have proven valuable in the locating, tracking, and studying of tropical storms. However, little progress has been made to date to utilize airborne sensors to measure and record oceanographic features (Wilkerson, 1966).

Despite its advantages, the use of airborne remote sensors has some serious limitations. Only surface and near surface phenomena can be detected. The marine atmosphere acts to deteriorate the signals that must pass through this medium. Water vapor and clouds are the primary factors causing reduced and distorted signals. High quality sea surface reference values of oceanographic elements

(ground truth) are required in the early phases of development to calibrate the remote sensed data and to evaluate sensors and sensing techniques. Arnold et al. (1967) have found that the lack of sufficient ground truth data that has hampered the efforts to date is largely due to the nonavailability of research vessels to support the work.

Earth Resources Aircraft Mission 79 was scheduled to overfly the area of the loop current (test site 173) about the time of cruise 68-A-8. The mission was actually flown September 10, 1968, five days after the cruise, using NASA aircraft 927 (a modified version of the Navy P3A patrol aircraft). The aircraft carried a metric camera (RC-8), an infrared imager (RS-7), and an infrared radiometer (Barnes PRT-5). The camera was used to examine the variation in appearance of the surface water and its relation to the different waters present between the central Gulf and the coastal areas as well as in the area of the loop current. The other two sensors were to detect thermal boundaries in the water and to measure the sea surface temperature respectively. The object of the flight was to acquire remotely sensed data over the Gulf of Mexico for the comparison with ground truth data taken by the R/V ALAMINOS and with data taken by the Nimbus III satellite. The ground truth measurements made by the R/V ALAMINOS are discussed in Chapter II.

Results

The mission was only of limited success from the standpoint of the R/V ALAMINOS ground truth comparisons. The aircraft track was to be a line from the NOMAD buoy (25.0°N and 90.0°W) to Tampa, Florida which coincided with transect five. (See Figure 1 for location.) Squall weather and clearance problems resulted in a departure from the aircraft's planned track. Data were gathered from an altitude of 5000 feet (1524 meters) for about three fourths of this transect. Weather in the vicinity of stations 70 and 71 prevented gathering any data while flying over the loop current in this area. A line of thunderstorms near stations 64 and 65 compromised the data in this area. The sea surface temperature gradients detected by classical methods and by the shipboard infrared thermometer were not apparent from the airborne sensors. This is attributed to the weather discussed above and to the fact that the change in surface temperature was at its lowest (0.3 to 0.5°C) at the eastern end of transect five. (See Figure 28 and Table II.)

Recommendations

The results of mission 79 were disappointing from the standpoint of detecting the oceanographic parameters that define the loop current. However, it is strongly recommended that further low level aircraft missions be flown over the loop current

(site 173) when they can be coordinated with research vessels that can provide adequate ground truth. The continuation of this phase of the SPOC program will help provide synoptic oceanographic data in the area of the loop current and will enhance the development of sensors (existing and nonexisting) to be carried in satellites and spacecraft.

Site 173 is an ideal location for this study. The Gulf of Mexico is surrounded by weather stations that can provide atmospheric soundings to define the medium that signals must pass through. A variety of oceanic regimes exists in this area that is convenient to MSC/NASA Houston, where the NASA aircraft is based, and Texas A & M University which operates a research vessel in this area. It is also an area in which a considerable amount of oceanographic research has been done in the past and is continuing today. The weather and flying conditions are favorable most of the year.

Cruise 68-A-8 found very good agreement in the values of sea surface temperature determined by various sensors including the shipboard infrared thermometer. The sea surface temperature data indicate that the sharp drop in sea surface temperature found at the loop current may be a good indication of this feature in the late summer. This feature was detected by the shipboard infrared thermometer. Plots of surface salinity (Figure 8) and dynamic topography (Figure 20) can also be used to depict the loop current and sensors to measure these parameters may be possible in the near

future (Paris, 1969). Leipper (1967) has reported that noticeable changes in sea state, surface films, and amounts of other drifting materials are sometimes found in the loop current. These features may be detected by photographic interpretation and radar techniques.

The Gulf Science Year will bring many outside investigators to the Gulf of Mexico next year. It would be an aid to this program to have additional remote sensed data available for participating investigators. During this program, many ships will be operating in the Gulf; and, with proper scheduling, they will be able to provide excellent ground truth coverage for aircraft missions. This influx of ships will temporarily eliminate the problem of insufficient vessels to provide ground truth in the SPOC program.

LIST OF REFERENCES

Arnold, J. E., L. R. A. Capurro, J. F. Paris, and D. Walsh, Ground truth requirements for remote sensing of oceanographic features, Unpubl. Rept. of the Dept. of Oceanogr., Texas A & M University, 1967.

Austin, G. B., Some recent oceanographic surveys of the Gulf of Mexico, Trans. Am. Geophys. Union, 36(5), 885-892, 1955.

Beyer, R. T., Formulas for sound velocity in sea water, J. Marine Res., 13(1), 113-121, 1954.

Birchett, J. A. K., Temperature-salinity relationships in the surface layers of the eastern Gulf of Mexico in August, 1966, Unpubl. M. S. thesis, Texas A & M University, May, 1967.

Carpenter, J. H., The Chesapeake Bay Institute Technique for the Winkler dissolved oxygen method, Limnol. and Oceanogr., 10(1), 141-143, 1965.

Cochrane, J. D., Investigations of the Yucatan Current, In unpubl. Rept. of the Dept. of Oceanogr. and Meteorol., The A & M College of Texas, Ref. 61-15F, 4-7, 1961.

Cochrane, J. D., Yucatan Current, In unpubl. Rept. of the Dept. of Oceanogr. and Meteorol., The A & M College of Texas, Ref. 63-18A, 6-11, 1963.

Cochrane, J. D., The Yucatan Current and Equatorial Currents of the western Atlantic, In unpubl. Rept. of the Dept. of Oceanogr. and Meteorol., Texas A & M University, Ref. 65-17T, 6-27, 1965.

Cochrane, J. D., The Yucatan Current, upwelling off northeastern Yucatan, and currents of waters of the western equatorial Atlantic, In unpubl. Rept. of the Dept. of Oceanogr. and Meteorol., Texas A & M University, Ref. 66-23T, 14-32, 1966.

Defant, A., Physical Oceanography, Vol. 1, 729 pp., Pergamon Press, London, 1961.

Dietrich, G., General Oceanography, 588 pp., Interscience Publishers, New York, N. Y., 1963.

Drennan, K. L., Surface circulation in the northeastern Gulf of Mexico, 116 pp., Gulf Research Laboratory, Oceanography Section, Technical Report #1, 1963.

Franceschini, G. A., Air-sea interaction study, In unpubl. Rept. of the Dept. of Oceanogr. and Meteorol., Texas A & M University, Ref. 66-23T, 33-35, 1966.

Gordon, A. L., Circulation in the Caribbean Sea, J. Geophys. Res., 72(24), 6207-6223, 1967.

Green, E. J., and D. F. Carritt, New tables for oxygen saturation of seawater, J. Marine Res., 25(2), 140-147, 1967.

Horton, J. W., Fundamentals of Sonar, 417 pp., U. S. Naval Institute, Annapolis, Maryland, 1961.

Hubertz, J. M., A study of the loop current in the eastern Gulf of Mexico, Unpubl. M. S. thesis, Texas A & M University, May, 1967.

Leipper, D. F., Physical oceanography of the Gulf of Mexico, Fishery Bulletin No. 89, U. S. Fish and Wildlife Service, Vol. 55, 119-137, 1954.

Leipper, D. F., A sequence of current patterns in the Gulf of Mexico, Unpubl. Rept. of the Dept. of Oceanogr., Texas A & M University, Ref. 67-9, 1967.

Leipper, D. F., Hydrographic station data, Gulf of Mexico, August-November Nansen casts, 1965-1967, Unpubl. Rept. of the Dept. of Oceanogr., Texas A & M University, Ref. 68-13T, 1968a.

Leipper, D. F., Hydrographic station data, Gulf of Mexico, August-November STD, 1965-1967, Unpubl. Rept. of the Dept. of Oceanogr., Texas A & M University, Ref. 68-14T, 1968b.

Leipper, D. F., Hydrographic station data, Gulf of Mexico, February-March Nansen casts, 1965-1968, Unpubl. Rept. of the Dept. of Oceanogr., Texas A & M University, Ref. 68-15T, 1968c.

Leipper, D. F., Hydrographic station data, Gulf of Mexico, February-April STD, 1967-1968, Unpubl. Rept. of the Dept. of Oceanogr., Texas A & M University, Ref. 68-16T, 1968d.

Leipper, D. F., Hydrographic station data, Gulf of Mexico, August 17-September 5, 1968, Nansen casts and STD, Unpubl. Rept. of the Dept. of Oceanogr., Ref. 68-17T, 1968e.

McLellan, H. J., Elements of Physical Oceanography, 146 pp., Pergamon Press, New York, N. Y., 1965.

Neuman, G., and W. J. Pierson, Jr., Principles of Physical Oceanography, 545 pp., Prentice-Hall Inc., Englewood Cliffs, N. J., 1966.

Nowlin, W. D., J. M. Hubertz, and R. O. Reid, A detached eddy in the Gulf of Mexico, J. Marine Res., 26(2), 185-186, 1967.

Nowlin, W. D., and H. J. McLellan, A characterization of the Gulf of Mexico waters in winter, J. Marine Res., 25(1), 29-59, 1967.

Paris, J. F., Microwave radiometry and its application to marine meteorology and oceanography, Unpubl. Rept. of the Dept. of Oceanogr., Texas A & M University, Ref. 69-1T, 1969.

Roll, H. U., Physics of the Marine Atmosphere, 426 pp., Academic Press, New York, N. Y., 1965.

Ryan, T. V., and P. J. Grim, A new technique for echo sounding corrections, International Hydrographic Review, 45(2), 41-58, 1968.

Schmitz, W. J., and W. S. Richardson, On the transport of the Florida Current, Deep-Sea Res., 15(6), 679-693, 1968.

Seiwell, H. R., Application of the distribution of oxygen to the physical oceanography of the Caribbean Sea region, Papers in Phys. Oceanogr. and Meteorol., 6(1), 1938.

Sower, L. A., Sound velocity formulas, Informal Oceanographic Manuscript No. 30-61, U. S. Naval Oceanographic Office, December, 1961.

Stommel, H., The Gulf Stream, second edition, 243 pp., University of California Press, 1965.

Sverdrup, H. U., M. W. Johnson, and R. H. Fleming, The Oceans; Their Physics, Chemistry, and General Biology, 1087 pp., Prentice-Hall, Englewood Cliffs, N. J., 1942.

Tucker, D. G., and B. K. Gazey, Applied Underwater Acoustics, 239 pp., Pergamon Press, London, 1966.

U. S. Naval Oceanographic Office, Historical environmental data, Gulf of Mexico, Area 18, June, 1967.

U. S. Naval Oceanographic Office, Atlas of pilot charts, Central American waters and South Atlantic Ocean, second edition, H. O. Pub. No. 106 (formerly H. O. Pub. No. 576), 1955.

U. S. Naval Oceanographic Office, Oceanographic atlas of the North Atlantic Ocean, Section I, Tides and Currents, H. O. Pub. No. 700, 1965.

Van Schuyler, P., and A. A. Hunger, A volume scattering and oceanographic study of an area in the eastern Gulf of Mexico, U. S. Naval Oceanographic Office, Informal Rept. No. 67-34, May, 1967.

Wilkerson, J. W., Airborne Oceanography, Geo-Marine Technology, 2(8), 9-16, 1966.

Wolff, P. M., L. P. Carstensen, and T. Laevastu, Analysis and forecasting of sea surface temperature, Fleet Numerical Weather Facility Technical Note 8, 26 February 1965.

Wust, G., Stratification and Circulation in the Antillean-Caribbean Basins, Pt. 1, 201 pp., Columbia University Press, New York, N. Y., 1964.

VITA

Lieutenant Michael J. Schneider

Born:

September 10, 1939 at Summit, New Jersey

Parents:

John H. and Mary J. Schneider

Education:

U. S. Merchant Marine Academy, 1957 - 1961, B. S. in Nautical Science (summa cum laude) July, 1961.

Professional Experience:

Commissioned as Ensign, USN, in July, 1961 and served in the Navy continuously since August, 1961.

Permanent Address:

M. J. Schneider
7 Westridge Road
Cooperstown, New York 13326

This thesis was typed by Mrs. June Hagler.